The Abdus Salam International Centre for Theoretical Physics

United Nations Educational, Scientific and Cultural Organization

IAEA International Atomic Energy Agency

SMR/1842-4

International Workshop on QCD at Cosmic Energies III

28 May - 1 June, 2007

Studies of Interaction Models at Energies Suitable for Neutrino Telescopes

T. Montaruli

University of Wisconsin-Madison
U S A

Strada Costiera 11, 34014 Trieste, Italy - Tel. +39 040 2240 111; Fax +39 040 224 163 - sci_info@ictp.it, www.ictp.it

Studies of interaction at energies suitable for Neutrino Telescopes

QCD @ Cosmic Energies III

- A talk on our struggles...
- Work with Patrick Berghaus, John Kelley, Newt Ganugapati, Yolanda Sestayo, at University of Wisconsin - Madison
- Thanks also to Johannes Ranft, Henrike Wissing, Athina Meli and Giuseppe Battistoni

Contents

- Neutrino Telescopes (NT) physics issues
- Short update on on NTs under construction
- Atmospheric neutrinos and muons: the largest rates ever recorded and the main backgrounds
- The impact of CR composition and of interaction models on atmospheric neutrino and muon simulations

Current Status of Neutrino Telescopes

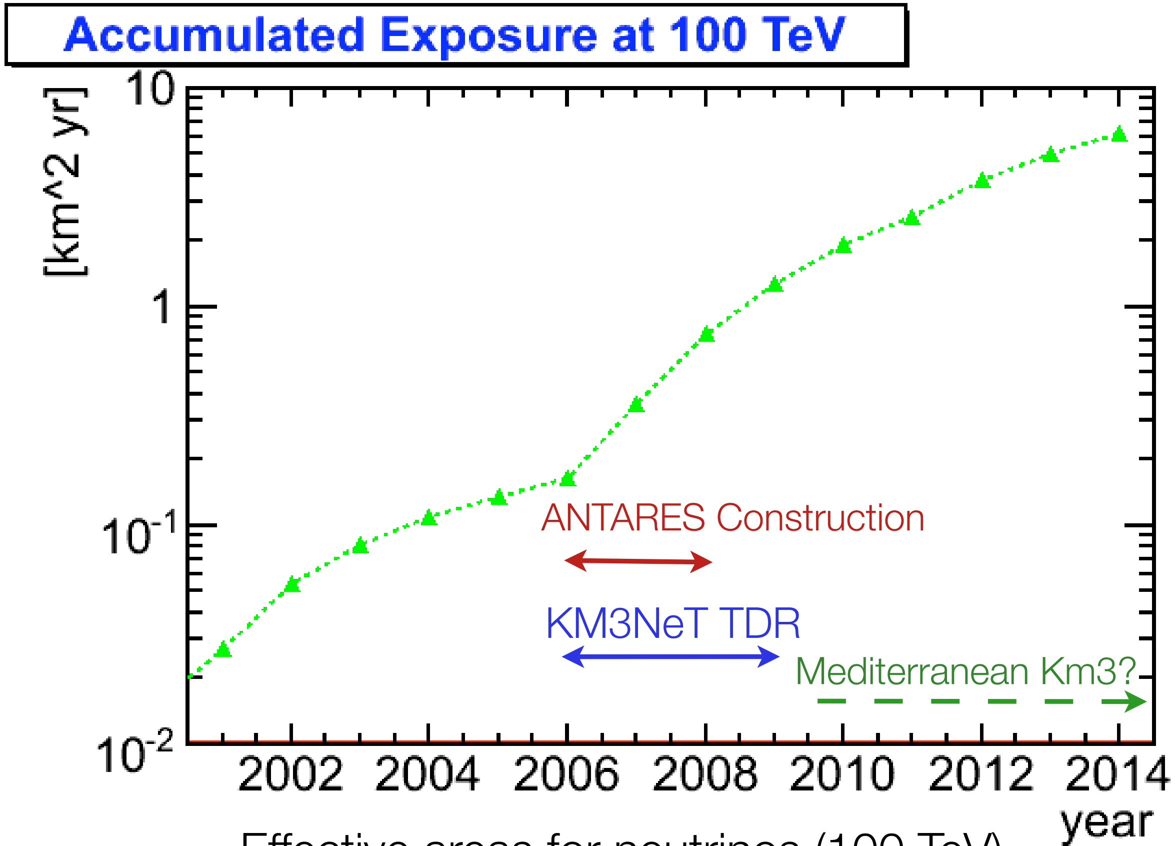

Effective areas for neutrinos (100 TeV)

AMANDA-II≈ANTARES≈IC9≈5 m^2

IC22≈30 m^2

IC80≈100 m^2

Status of IceCube Observatory 2007

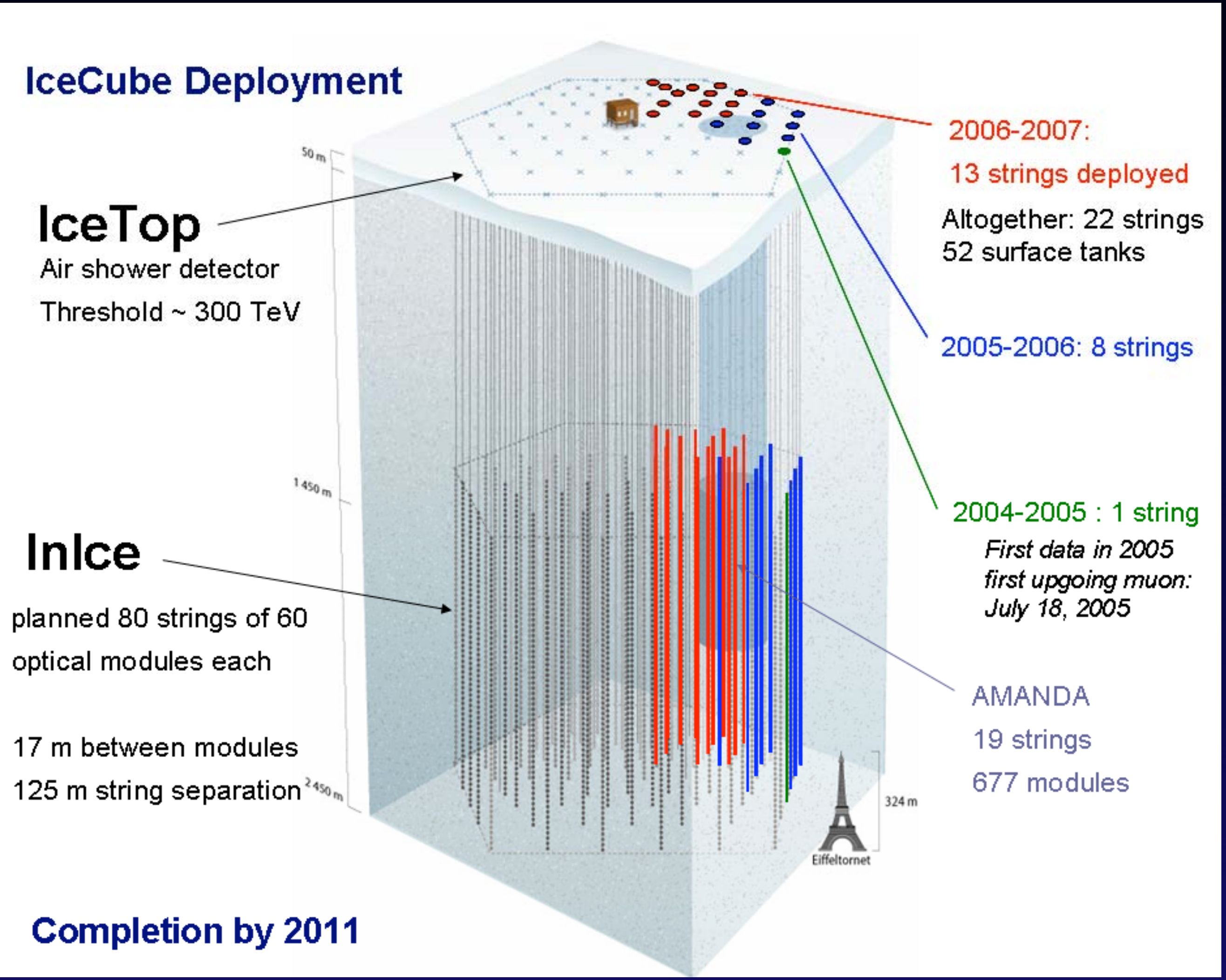

IceCube array

70+ strings and IceTop stations planned

22 strings and 1320 DOMs installed

26 IceTop stations with 104 DOMs installed

1424 DOMs in 2007
only 1.1% are not usable
1.3% have minor issues that can be solved

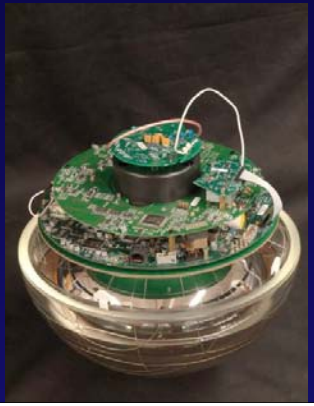

One of the first event with 22 strings

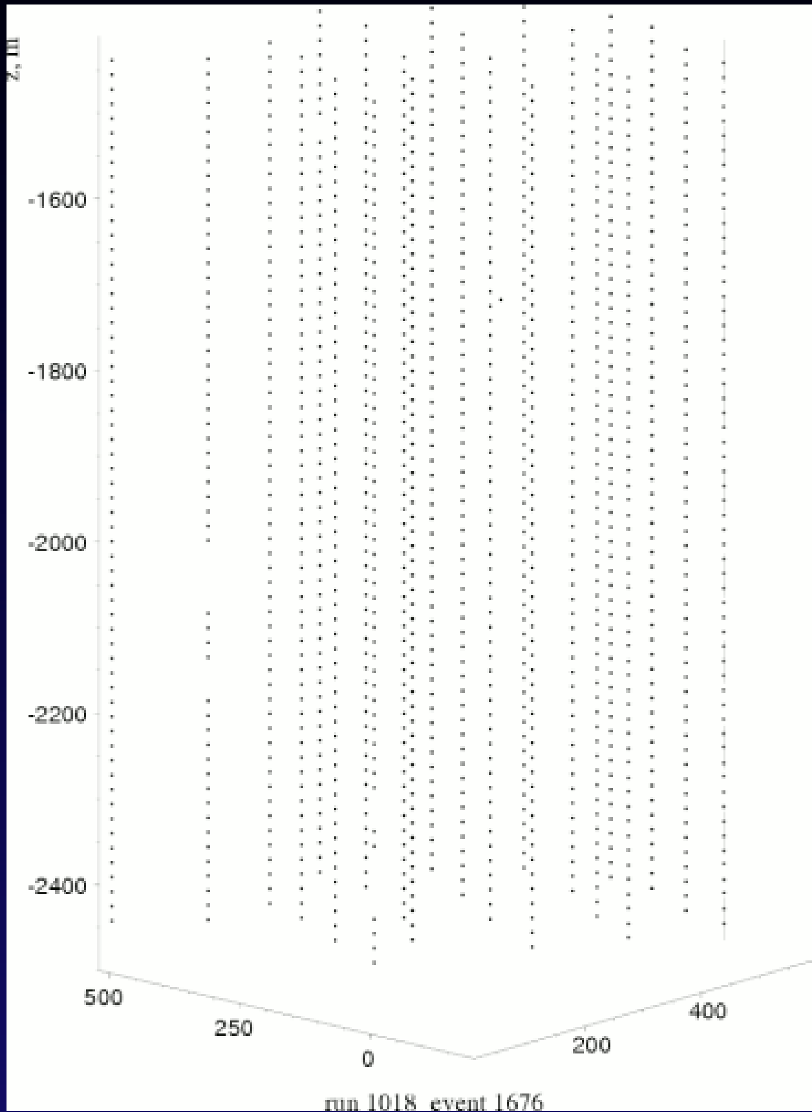

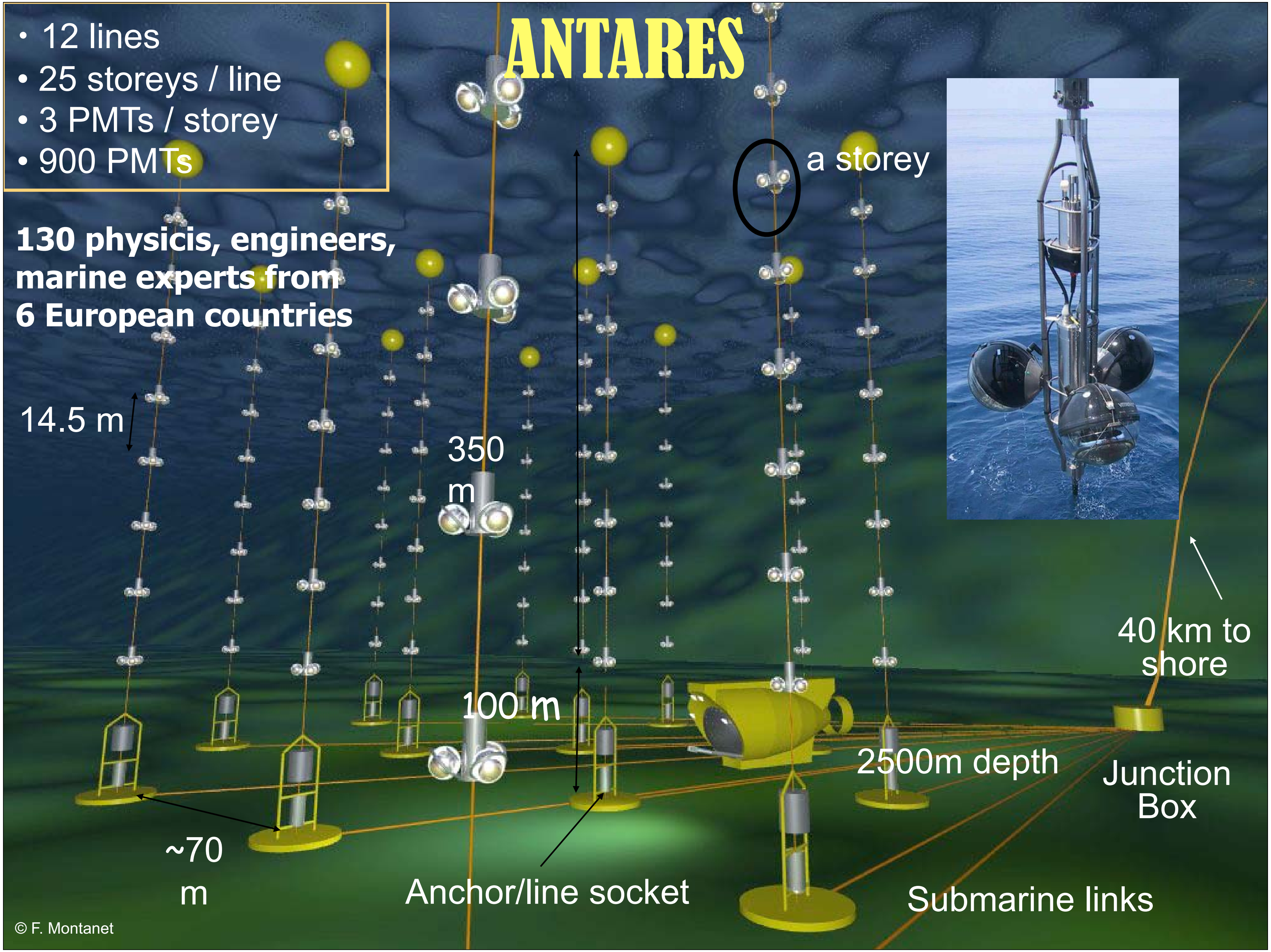
ANTARES
• 12 lines
• 25 storeys / line
• 3 PMTs / storey
• 900 PMTs
130 physicis, engineers, marine experts from 6 European countries
a storey
14.5 m
350 m
100 m
40 km to shore
2500m depth
Junction Box
~70 m
Anchor/line socket
Submarine links
© F. Montanet

Building lines in the sea: ANTARES

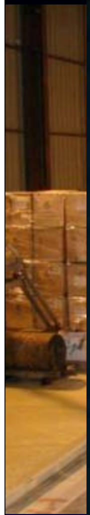
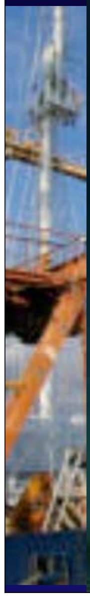
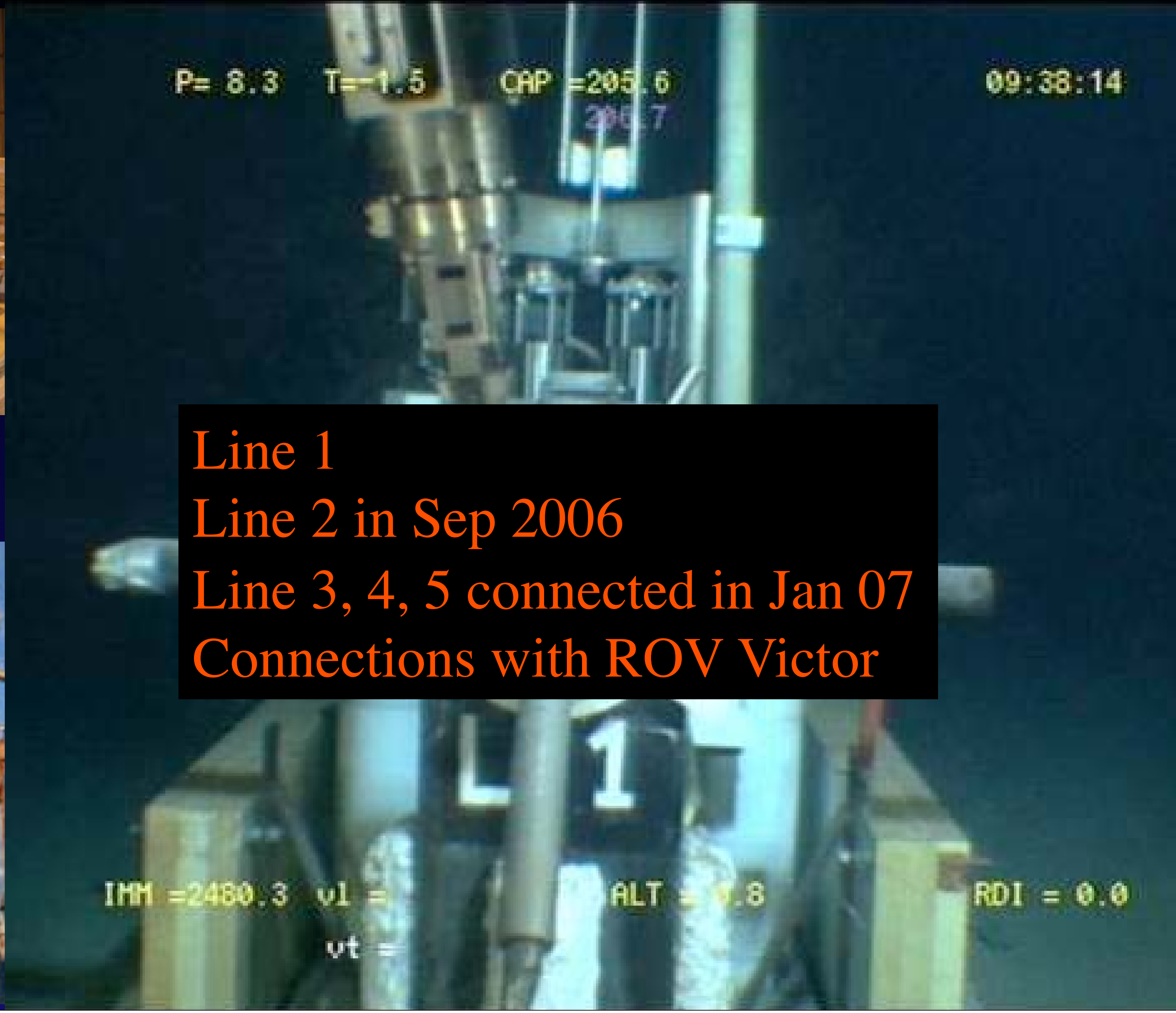

Line 1
Line 2 in Sep 2006
Line 3, 4, 5 connected in Jan 07
Connections with ROV Victor

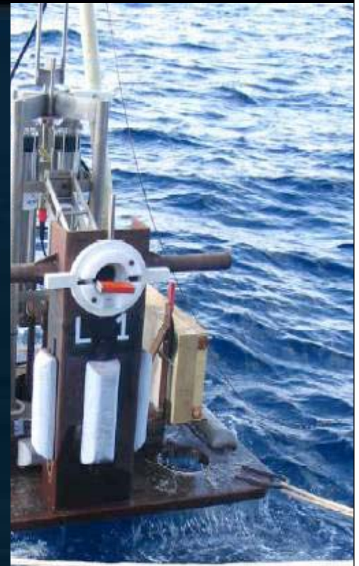

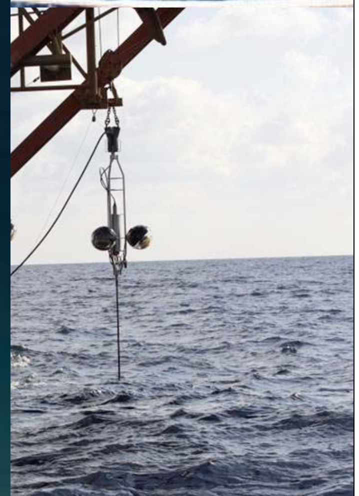


Events with 5 lines!

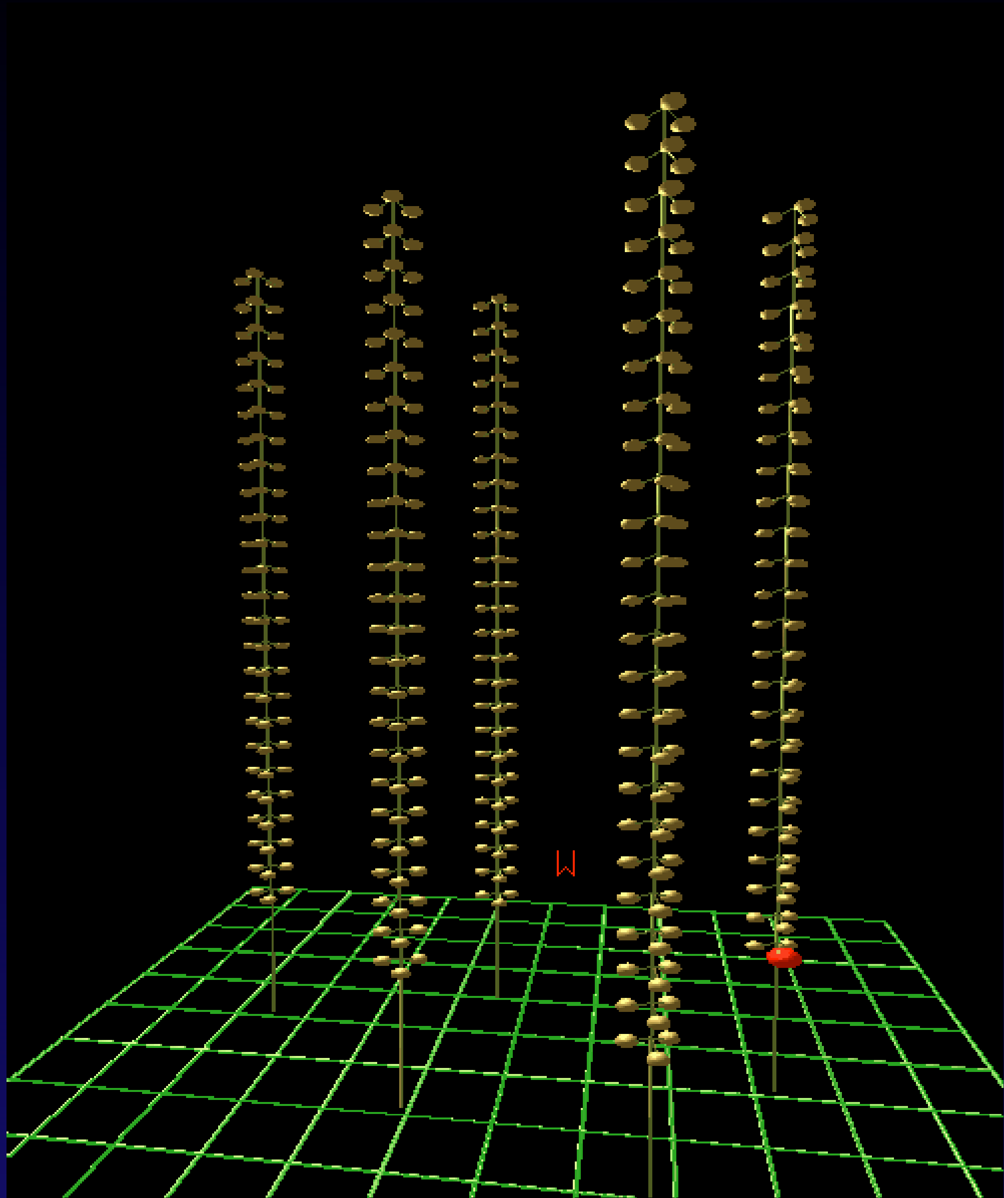

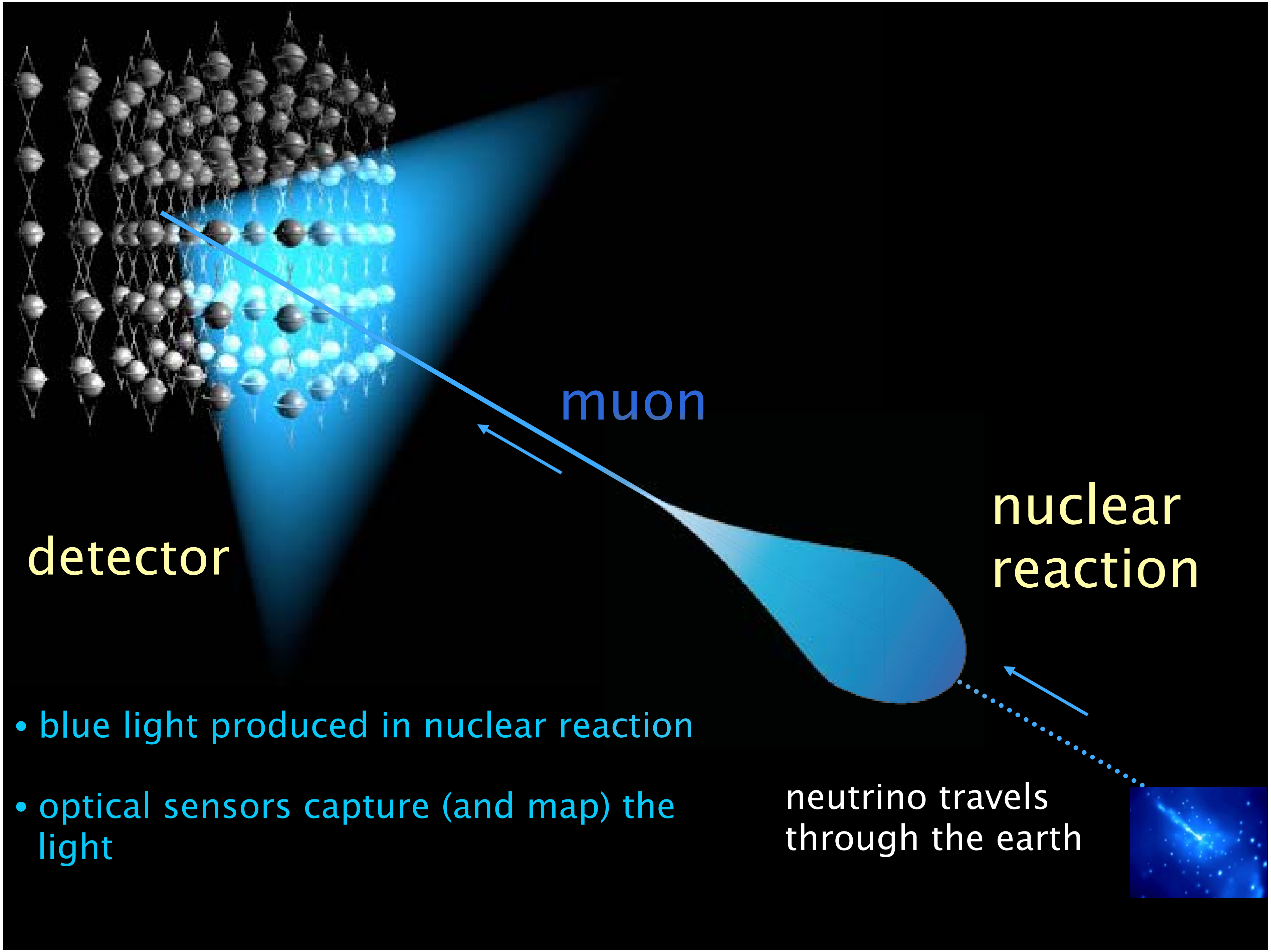
muon
nuclear reaction
detector
• blue light produced in nuclear reaction
• optical sensors capture (and map) the light
neutrino travels through the earth

Neutrino Topologies

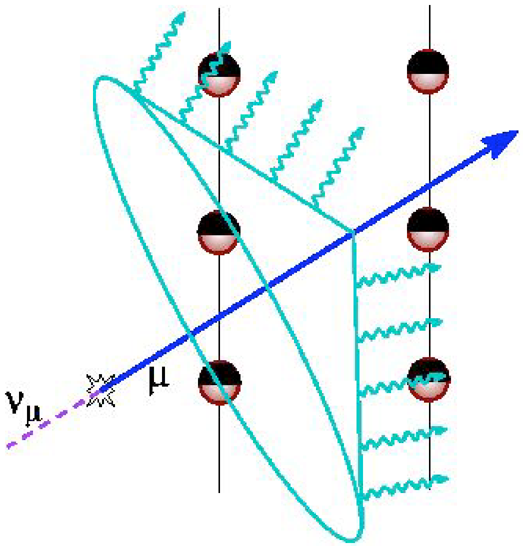

Muon neutrino

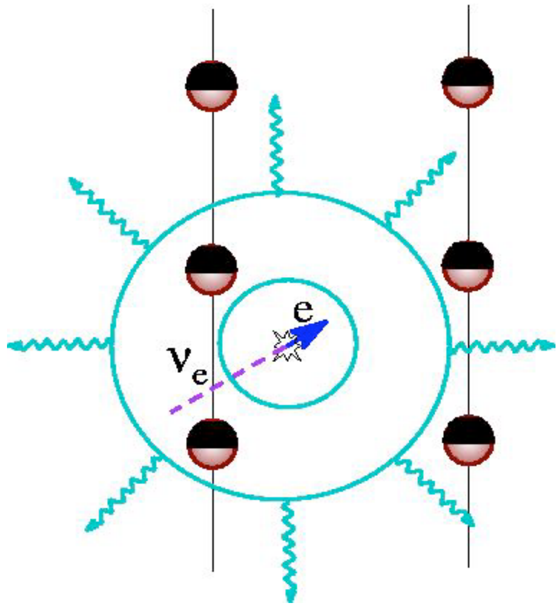

Electron neutrino

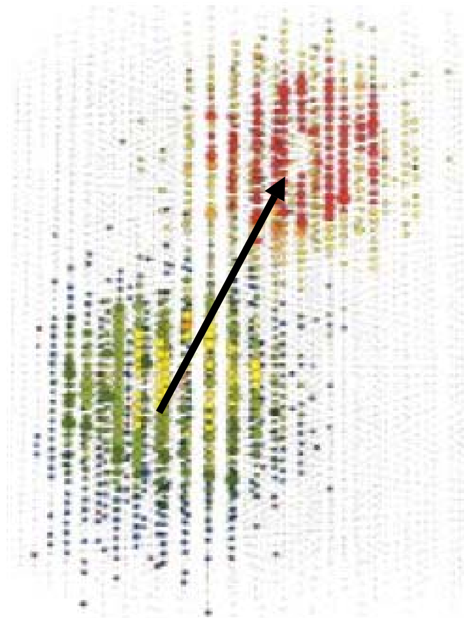

Tau neutrino

Messengers from the Universe

- Straight line propagation to point back to sources
- Small absorption in sources and during propagation

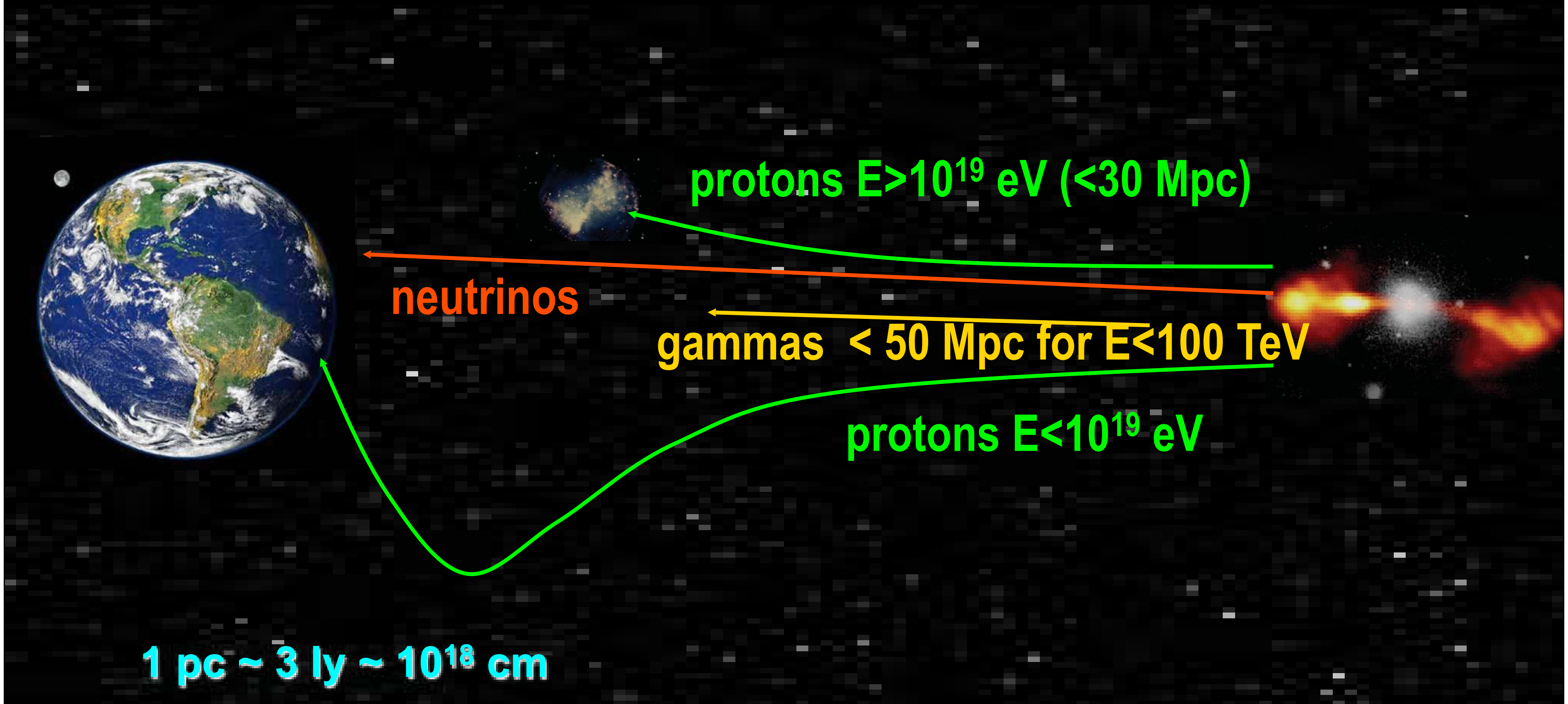

Neutrino sources @ > 100 GeV

Astrophysical Accelerators

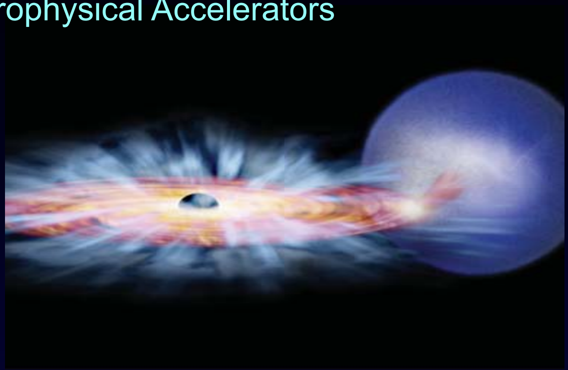

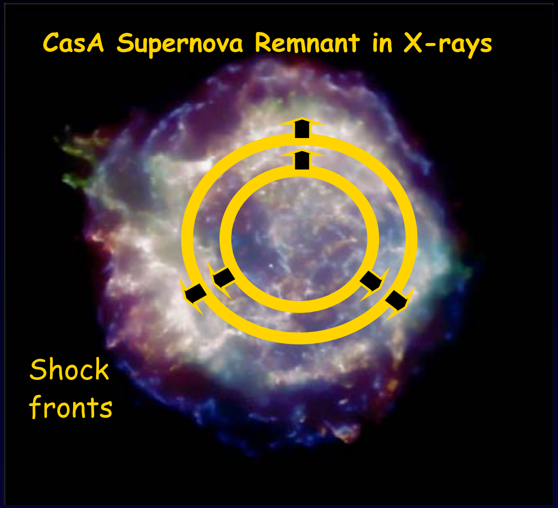

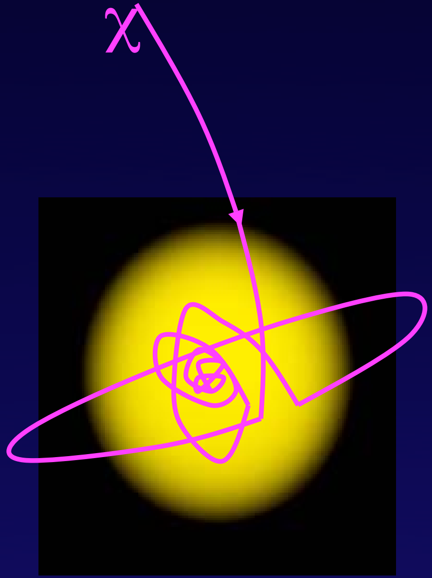

DM annihilation

Cosmic Rays on atmosphere and on ISM or during propagation on CMB

Neutrinos allow for observation of '**hidden regions**' (BH, pulsars, initial epochs of SN explosions,...).
The penetrating power of νs is important also for **moderately opaque sources** from which we may be seeing ϒ *spectra that are significantly distorted*

Neutrino production

Beam-dump model: $\pi^0 \rightarrow \gamma$-astronomy $\pi^\pm \rightarrow \nu$-astronomy

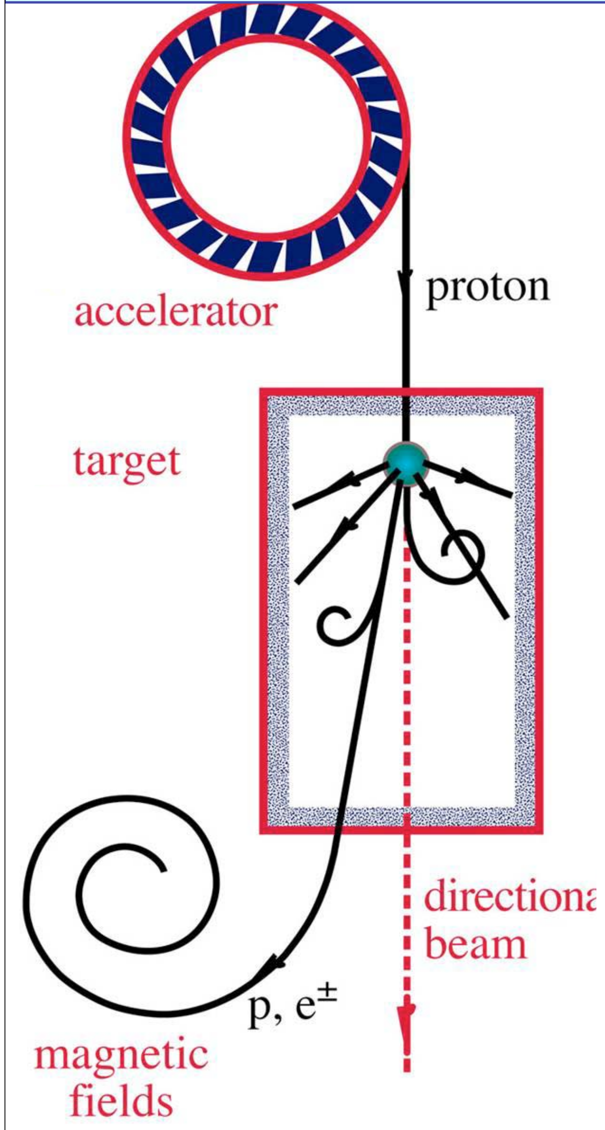

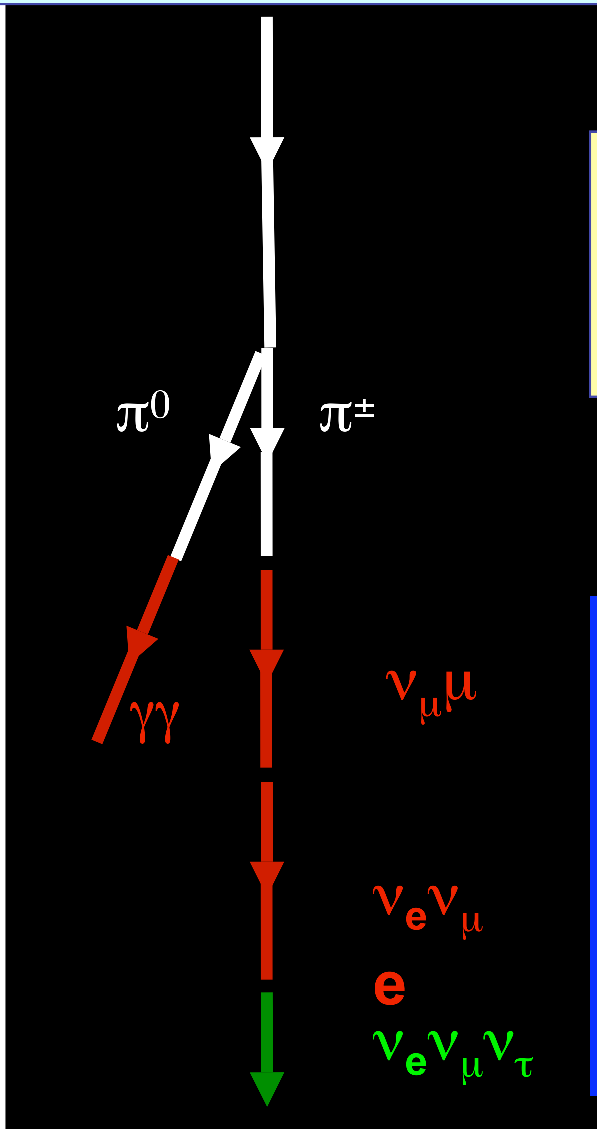

Neglecting γ absorption

$\varphi_\nu \sim \varphi_\gamma$

Targets: p or ambient γ

initial fluxes are

$\varphi_{\nu_e} : \varphi_{\nu_\mu} : \varphi_{\nu_\tau} = 1:2:0$

after oscillations

$\varphi_{\nu_e} : \varphi_{\nu_\mu} : \varphi_{\nu_\tau} = 1:1:1$

The many upper bounds and km3 potential

➔ F_ν ~ 40 x Waxman-Bahcall at 10^{16} eV, comparable at 10^{19} eV

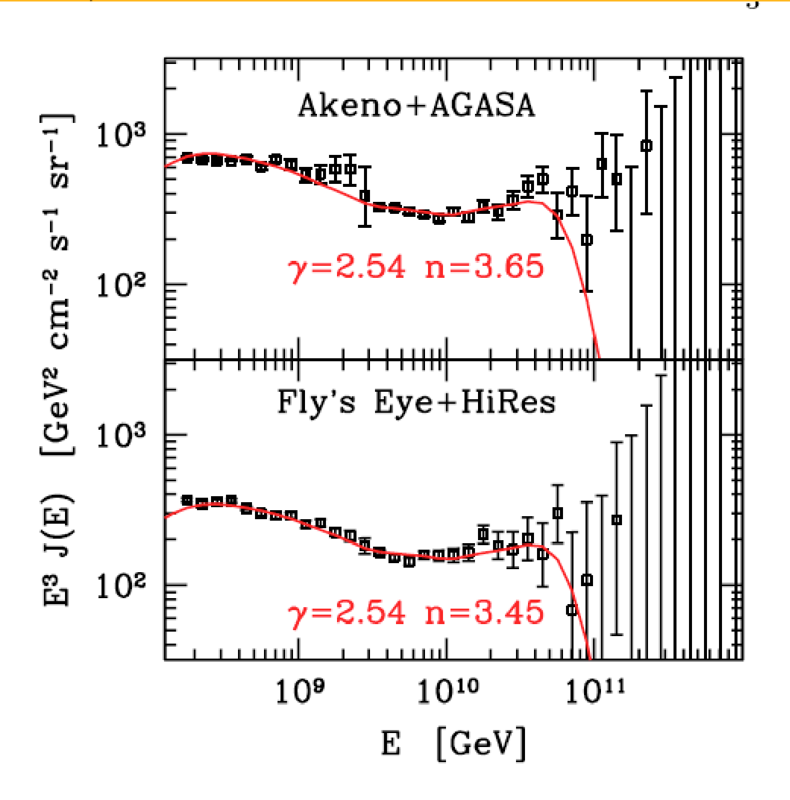

Index is 2.5, not 2.0

The composition and spectral shape of CRs above 10^{17} eV is relevant for UHE neutrinos

Optically thin sources using AGASA and HiReS spectra and W&B limit

IceCube 10 yrs

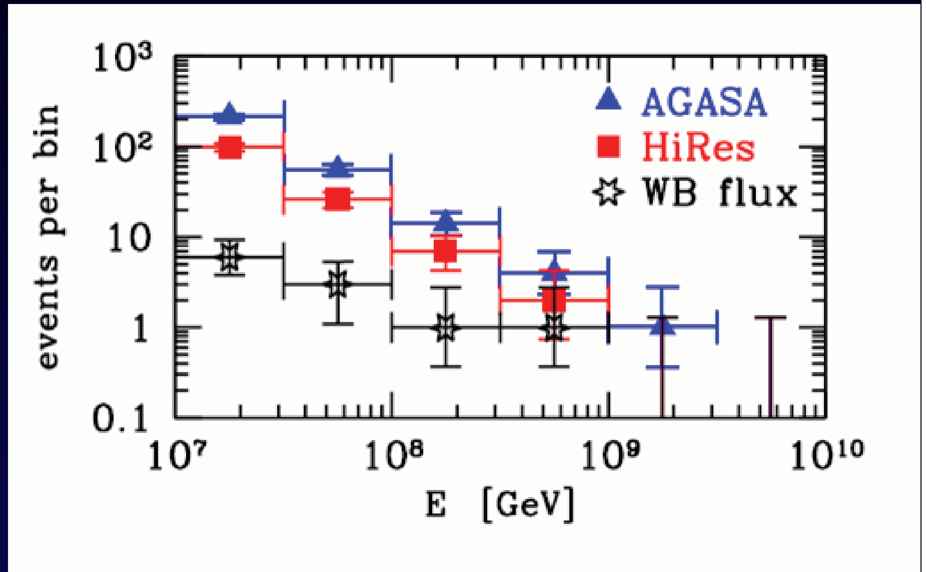

Ahlers et al 2005 is in the range of sensitivity for AMANDA-II

Composition at UHE

EPOS, Werner Liu Pierog, Phys Rev C 74 (2005)

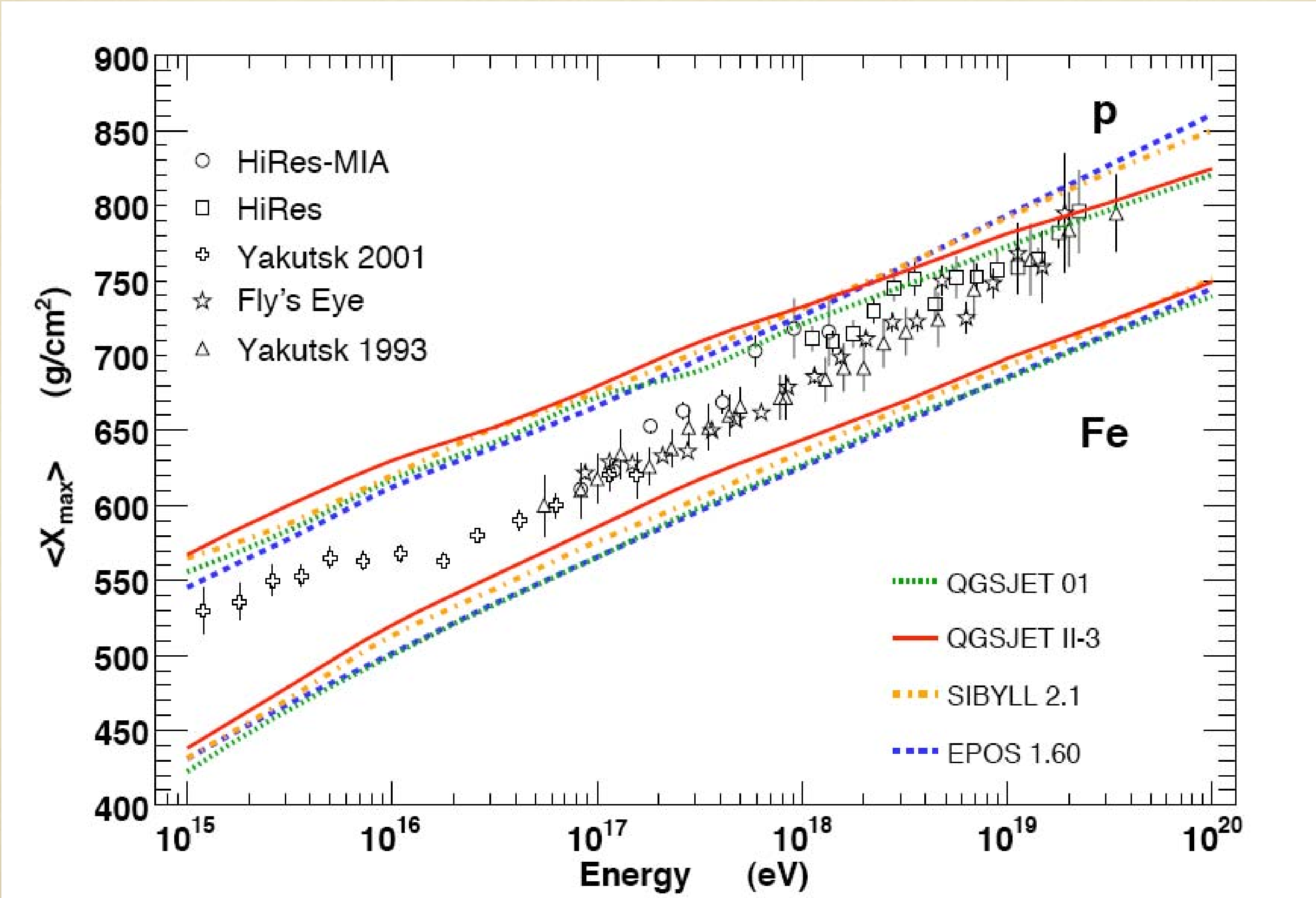

Atmospheric showers

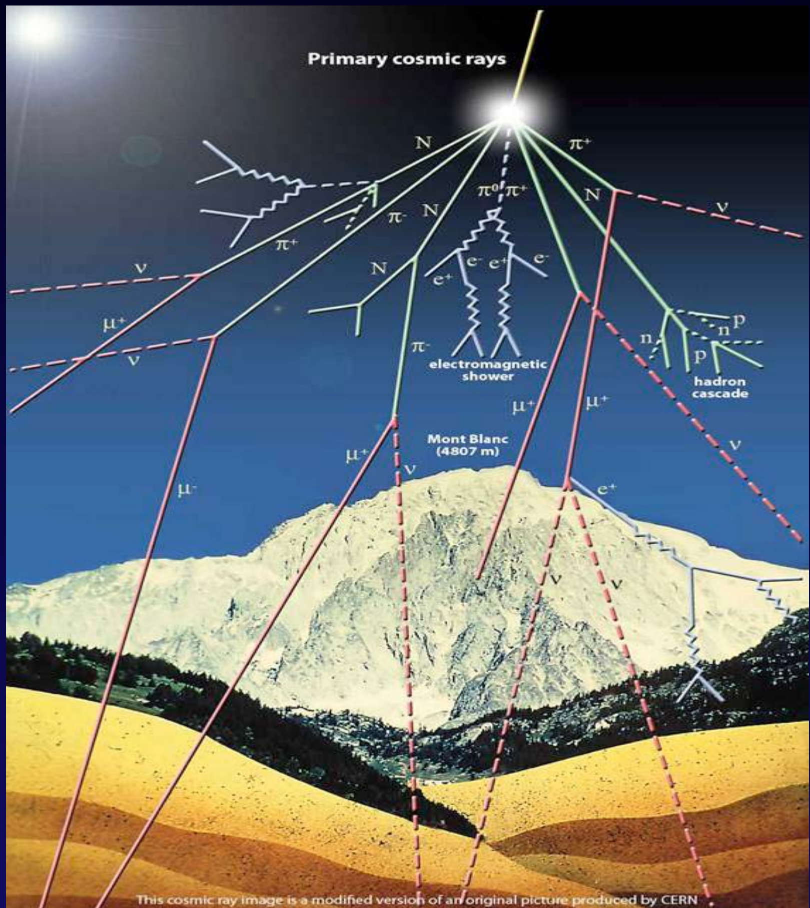

Mass oscillations are
a small effect in AMANDA/
IceCube
(< 10%)
In ANTARES observation is made difficult due to optical backgrounds that reduce the efficiency at low energies

INTERACTION AND PROPAGATION CODES

We used:

- CORSIKA 6321 and CORSIKA 6600
- D.Heck, T. Pierog, J. Knapp, CORSIKA: an air shower simulation program, www-ik.fzk.de/corsika
- FLUKA2007: A. Fassò et al., FLUKA: a multi-particle transport code, CERN-2005-10, www.fluka.org
- DPMJET 2.55 J. Ranft, PRD51 (1995) 64, hep-ph/9911213, hep-ph/9911232
- QGSJET01-02 Ostapchenko, PRD 74 (2006) 014026 and ref
- SIBYLL Fletcher, Gaisser Lipari, Stanev, PRD50 (1994) 5710

Atmospheric shower simulation in NT

- In AMANDA/ANTARES scale detector UHE analyses mainly sensitive to 10^{19} eV (Peak @ about 10^{16} eV)
- CORSIKA air shower development code
- CR composition: Wiebel-Sooth superseeded by Hörandel ($Z*E_H$ knee dependence)
- Hadronic model: not enough muons in AMANDA. Changed QGSJET01 to SIBYLL

AMANDA primary energy distribution (by Henrike Wissing)

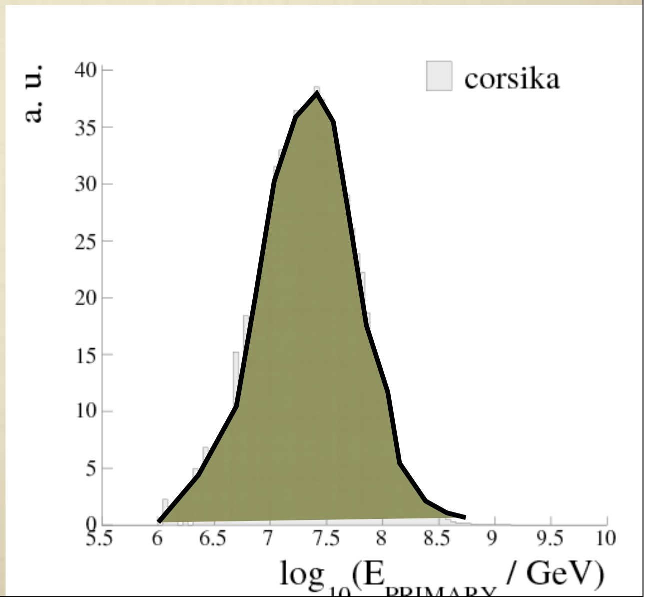

UHE analysis sensitivity to CR composition

Hörandel vs 2 component model (Glasstetter et al., also tuned on KASCADE - 80% Fe @ 10^{17} eV)

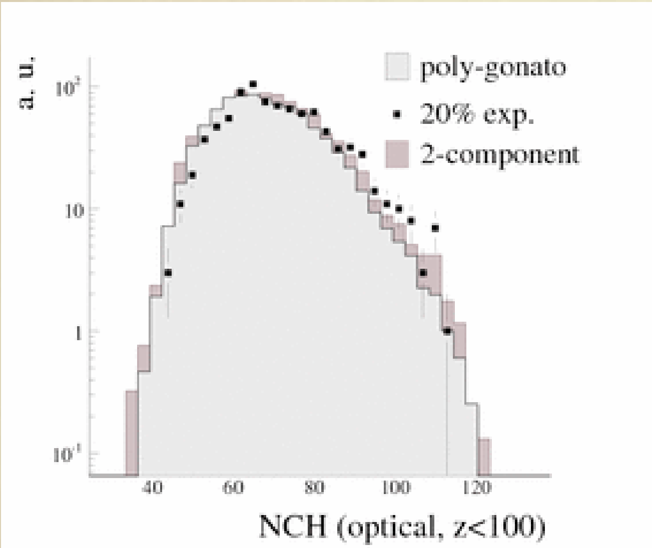

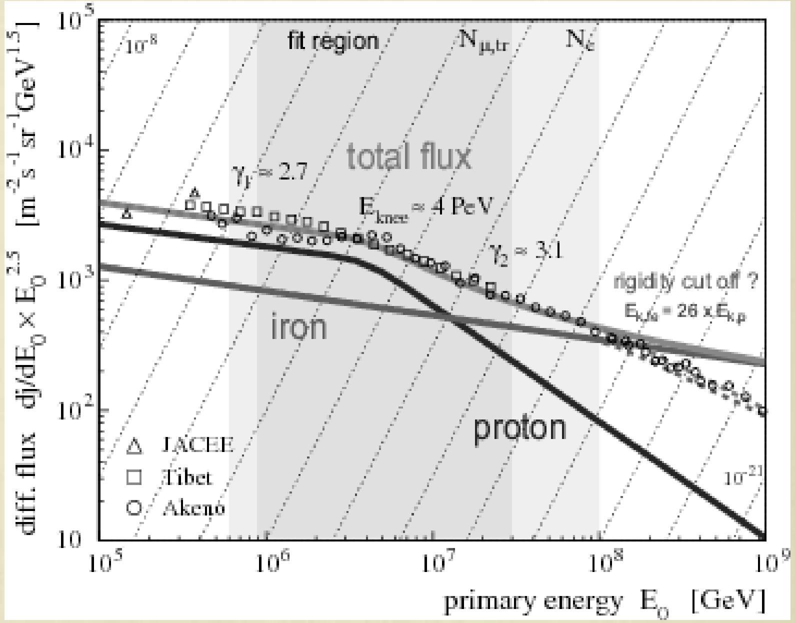

- By Henrike WISSING, Monopole ANalysis, Preliminary

The CR composition

Available online at www.sciencedirect.com
SCIENCE DIRECT®
Astroparticle Physics 19 (2003) 193–220
ELSEVIER
Astroparticle Physics
www.elsevier.com/locate/astropart

On the knee in the energy spectrum of cosmic rays

Jörg R. Hörandel

Institut für Experimentelle Kernphysik, University of Karlsruhe, P.O. Box 3640, 76021 Karlsruhe, Germany

Received 15 April 2002; received in revised form 26 July 2002; accepted 6 August 2002

Abstract

The *knee* in the all-particle energy spectrum is scrutinized with a phenomenological model, named *poly-gonato* model, linking results from direct and indirect measurements. For this purpose, recent results from direct and indirect measurements of cosmic rays in the energy range from 10 GeV up to 1 EeV are examined. The energy spectra of individual elements, as obtained by direct observations, are extrapolated to high energies using power laws and compared to all-particle spectra from air shower measurements. A cut-off for each element proportional to its charge Z is assumed. The model describes the knee in the all-particle energy spectrum as a result of subsequent cut-offs for individual elements, starting with the proton component at 4.5 PeV, and the second change of the spectral index around 0.4 EeV as due to the end of stable elements ($Z = 92$). The mass composition, extrapolated from direct measurements to high energies, using the poly-gonato model, is compatible with results from air shower experiments measuring the electromagnetic, muonic, and hadronic components. But it disagrees with the mass composition derived from X_{max} measurements using Čerenkov and fluorescence light detectors.

The Polygonato model

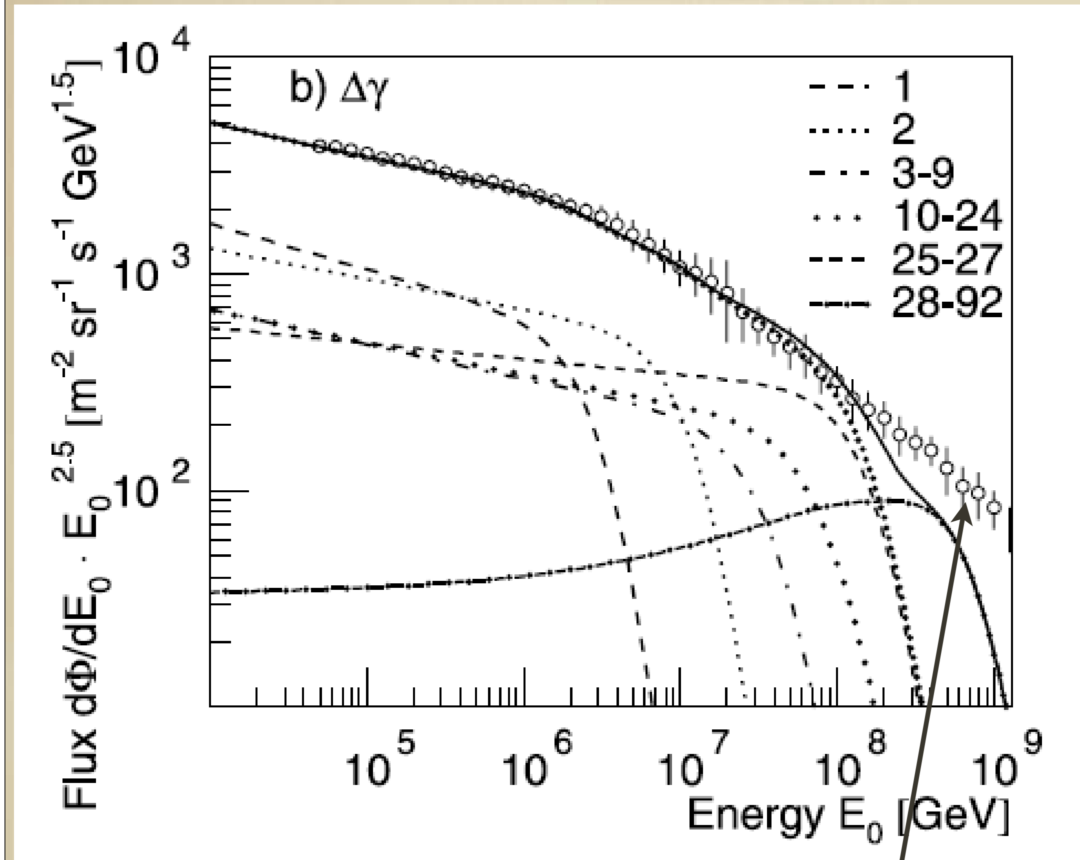

Absolute flux Φ_Z^0 $((\mathrm{m}^2\,\mathrm{sr\,s\,TeV})^{-1})$ at $E_0 = 1$ TeV/nucleus an

Z		Φ_Z^0	$-\gamma_Z$
1[a]	H	8.73×10^{-2}	2.71
2[a]	He	5.71×10^{-2}	2.64
3[b]	Li	2.08×10^{-3}	2.54
4[b]	Be	4.74×10^{-4}	2.75
5[b]	B	8.95×10^{-4}	2.95
6[b]	C	1.06×10^{-2}	2.66
7[b]	N	2.35×10^{-3}	2.72
8[b]	O	1.57×10^{-2}	2.68
9[b]	F	3.28×10^{-4}	2.69
10[b]	Ne	4.60×10^{-3}	2.64
11[b]	Na	7.54×10^{-4}	2.66
12[b]	Mg	8.01×10^{-3}	2.64
13[b]	Al	1.15×10^{-3}	2.66
14[b]	Si	7.96×10^{-3}	2.75
15[b]	P	2.70×10^{-4}	2.69
16[b]	S	2.29×10^{-3}	2.55
17[b]	Cl	2.94×10^{-4}	2.68
18[b]	Ar	8.36×10^{-4}	2.64
19[b]	K	5.36×10^{-4}	2.65
20[b]	Ca	1.47×10^{-3}	2.70
21[b]	Sc	3.04×10^{-4}	2.64
22[b]	Ti	1.14×10^{-3}	2.61
23[b]	V	6.31×10^{-4}	2.63
24[b]	Cr	1.36×10^{-3}	2.67
25[b]	Mn	1.35×10^{-3}	2.46
26[b]	Fe	2.04×10^{-2}	2.59

$$\frac{d\Phi}{dE_0}(E_0) = \sum_{Z=1}^{92} \frac{d\Phi_Z}{dE_0}(E_0)$$

All particle

Extragal component?

Simulation of the knee

- In simulations we are using a common difference Δγ between spectral indices below and above the knee instead of a common slope for all

Cut-off ($\widehat{E}_Z$)	Rigidity dependent ($\widehat{E}_p Z$)
$\widehat{E}_p$ (PeV)	4.51 ± 0.52
γ_c	-4.68 ± 0.23
ϵ_c	1.87 ± 0.18
χ^2/d.o.f.	0.116
$\widehat{E}_p$ (PeV)	4.49 ± 0.51
$\Delta\gamma$	2.10 ± 0.24
ϵ_c	1.90 ± 0.19
χ^2/d.o.f.	0.113

$$\frac{\mathrm{d}\Phi_Z}{\mathrm{d}E_0}(E_0) = \Phi_Z^0 E_0^{\gamma_Z}\left[1 + \left(\frac{E_0}{\widehat{E}_Z}\right)^{\epsilon_c}\right]^{\frac{-\Delta\gamma}{\epsilon_c}}$$

The Polygonato model

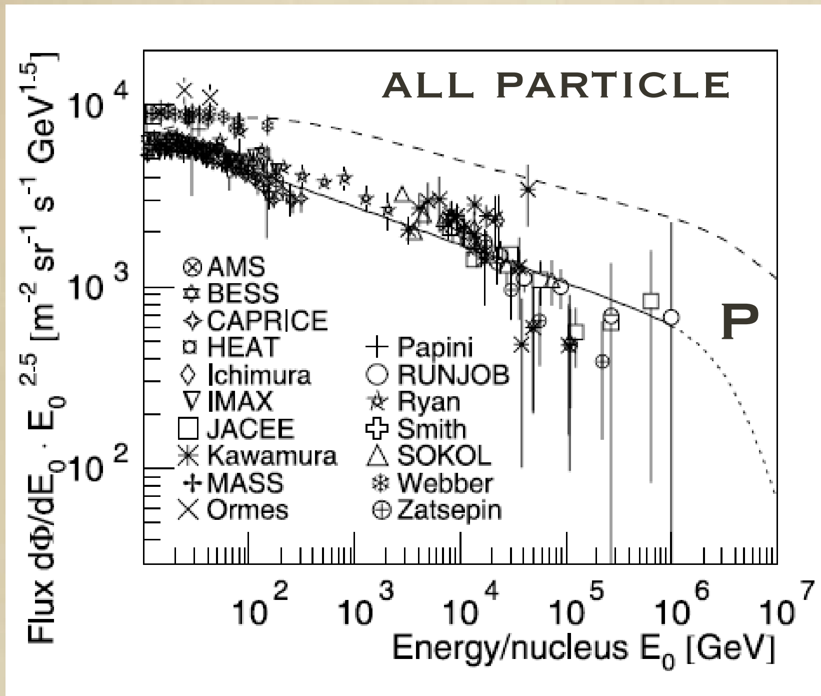

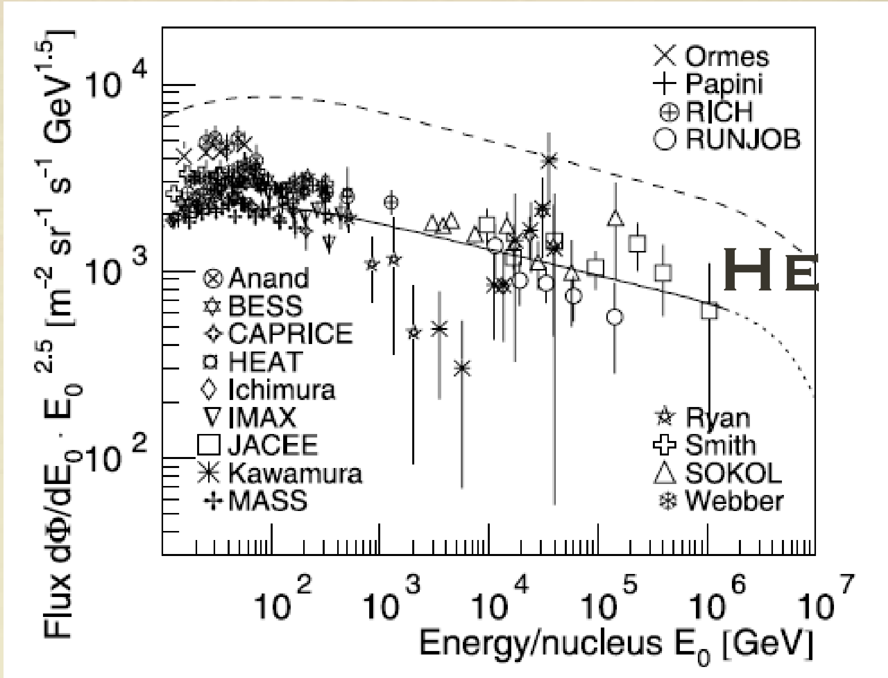

Protons are $E^{-2.71}$

Wiebel-Sooth steeper

$E^{-2.74}$

He same spectral index than W-S but 25% lower normalization

No differential data exist Z>28 so spectral index is extrapolated from lower Z elements

Above $10^{15.7}$ eV AKENO, Haverah park and Fly's EYE

Neutrino Measurement and CR composition

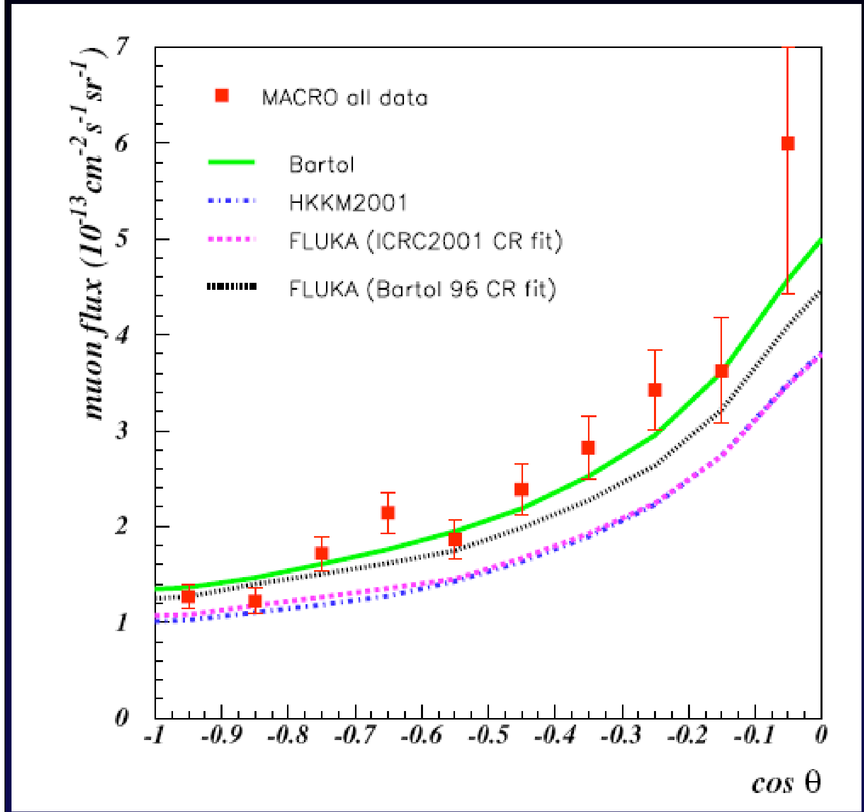

Throughgoing muons flux more compatible with p with $E^{-2.71}$ + hadronic models that produce lower amount of pions/kaons than TARGET (eg FLUKA or DPMJET-III vs Bartol group) or $E^{-2.74}$ and Bartol

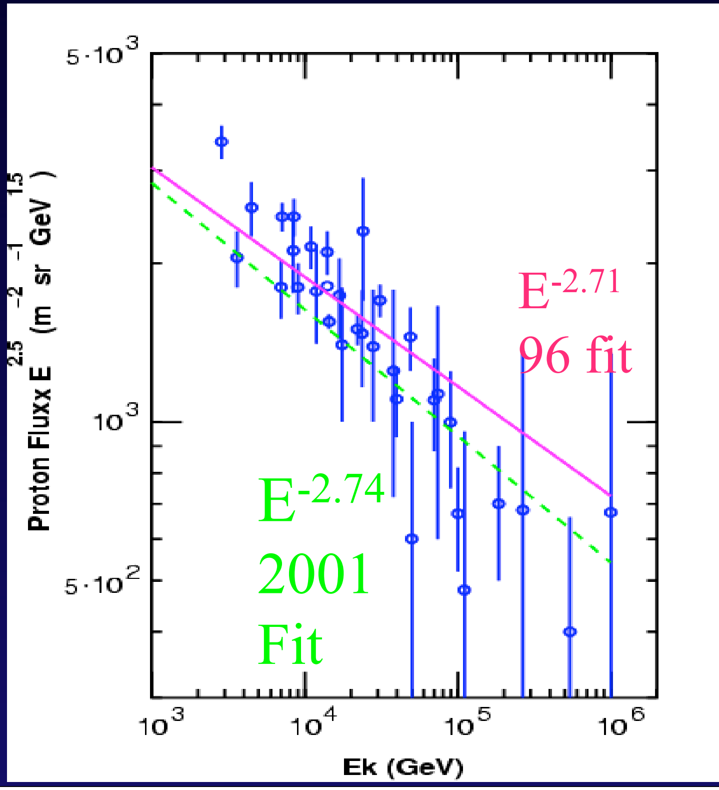

TM, ICRC2005 rapporteur talk and
Battistoni et al, ICRC2005
MACRO Final analysis, Eur. Phys. J. C36 (2004)

Possible composition at UHE

- sum all heavier nuclei into one only function to be used as Fe (we do not succeed in running heavier nuclei)

- simulate an extra-galactic p component and low transition as suggested by Hires

Hillas, 2005

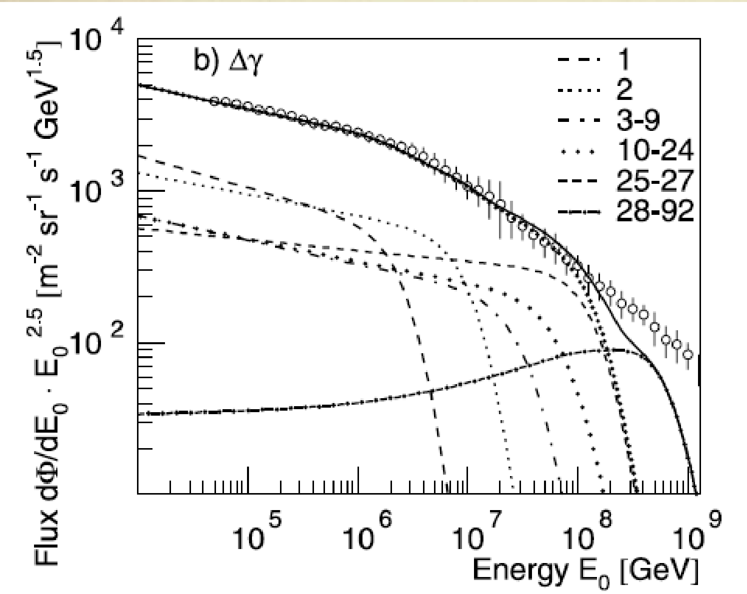

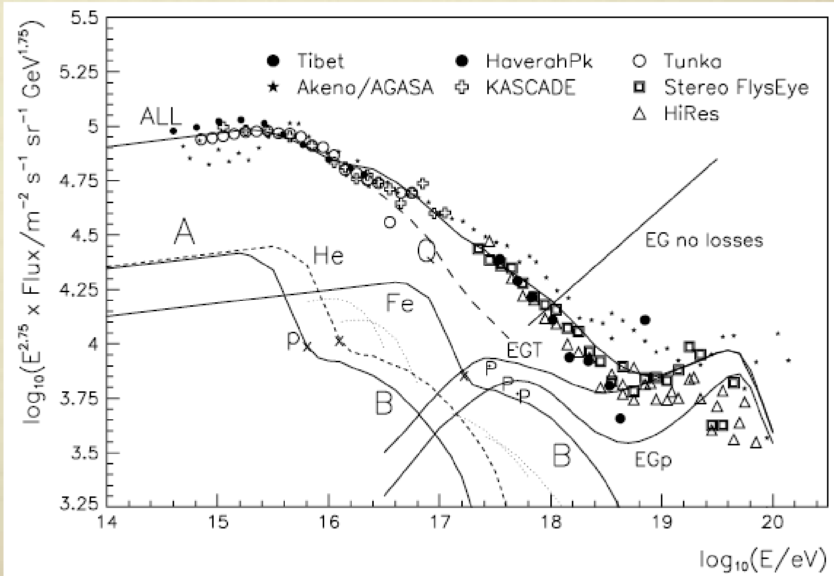

All-particle spectrum unfolding

Hadronic models and CR are highly correlated

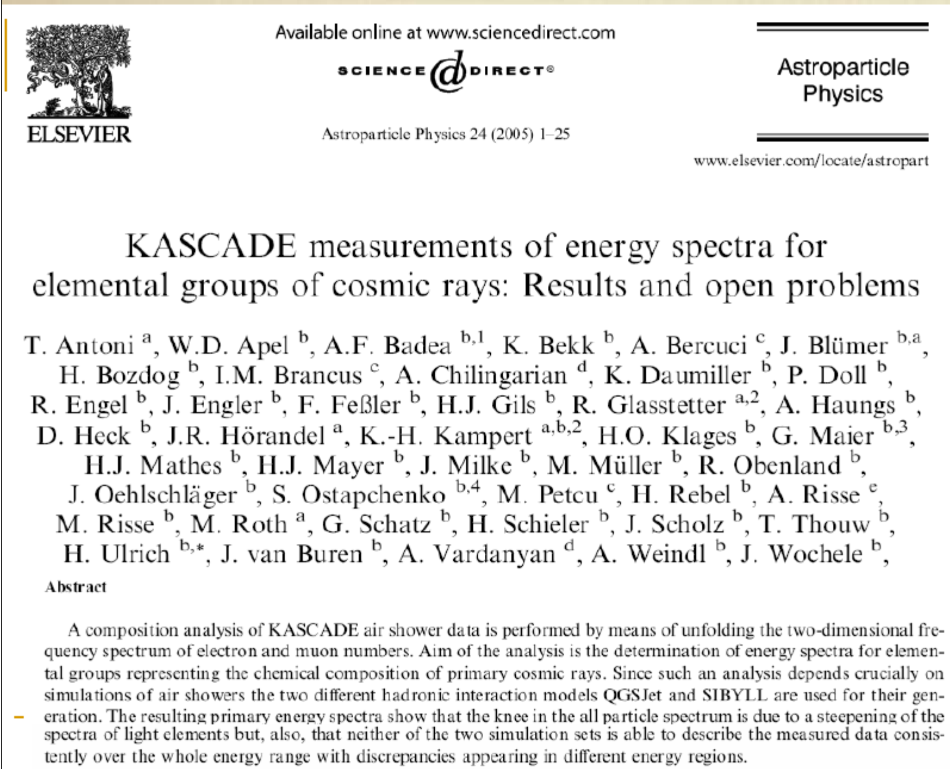

Available online at www.sciencedirect.com

SCIENCE DIRECT®

Astroparticle Physics 24 (2005) 1–25

Astroparticle Physics

www.elsevier.com/locate/astropart

ELSEVIER

KASCADE measurements of energy spectra for elemental groups of cosmic rays: Results and open problems

T. Antoni [a], W.D. Apel [b], A.F. Badea [b,1], K. Bekk [b], A. Bercuci [c], J. Blümer [b,a], H. Bozdog [b], I.M. Brancus [c], A. Chilingarian [d], K. Daumiller [b], P. Doll [b], R. Engel [b], J. Engler [b], F. Feßler [b], H.J. Gils [b], R. Glasstetter [a,2], A. Haungs [b], D. Heck [b], J.R. Hörandel [a], K.-H. Kampert [a,b,2], H.O. Klages [b], G. Maier [b,3], H.J. Mathes [b], H.J. Mayer [b], J. Milke [b], M. Müller [b], R. Obenland [b], J. Oehlschläger [b], S. Ostapchenko [b,4], M. Petcu [c], H. Rebel [b], A. Risse [e], M. Risse [b], M. Roth [a], G. Schatz [b], H. Schieler [b], J. Scholz [b], T. Thouw [b], H. Ulrich [b,*], J. van Buren [b], A. Vardanyan [d], A. Weindl [b], J. Wochele [b],

Abstract

A composition analysis of KASCADE air shower data is performed by means of unfolding the two-dimensional frequency spectrum of electron and muon numbers. Aim of the analysis is the determination of energy spectra for elemental groups representing the chemical composition of primary cosmic rays. Since such an analysis depends crucially on simulations of air showers the two different hadronic interaction models QGSJet and SIBYLL are used for their generation. The resulting primary energy spectra show that the knee in the all particle spectrum is due to a steepening of the spectra of light elements but, also, that neither of the two simulation sets is able to describe the measured data consistently over the whole energy range with discrepancies appearing in different energy regions.

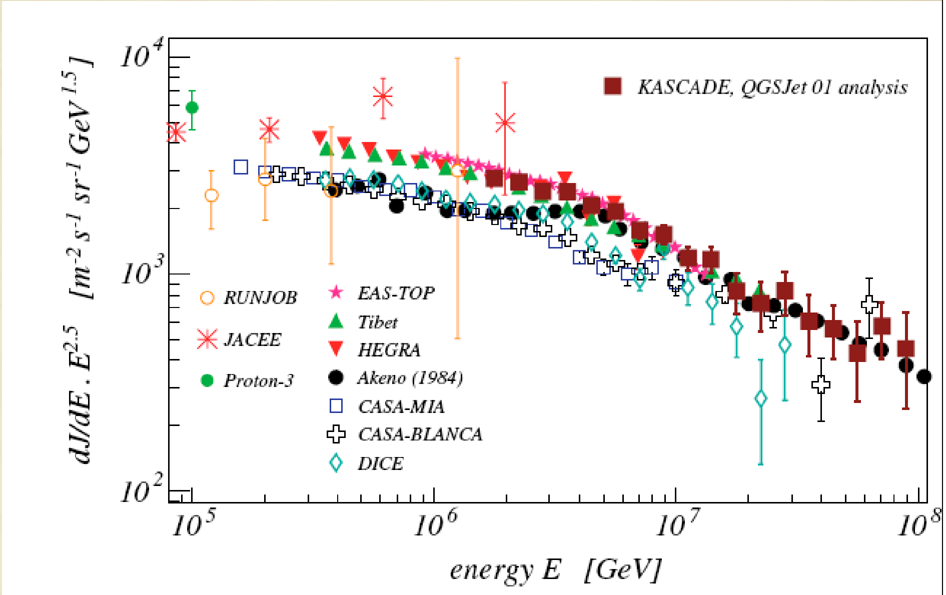

Unfolding of electron number N_e and N_μ at 40 and 200m to determine the energy spectra for different elemental groups

The hadronic models and KASCADE data at GROUND

All particle agrees for QGSJET-01 and Sibyll. QGSJET produces too many muons or too few electrons at low energies. Sibyll at high energy is too electron rich or too muon poor.

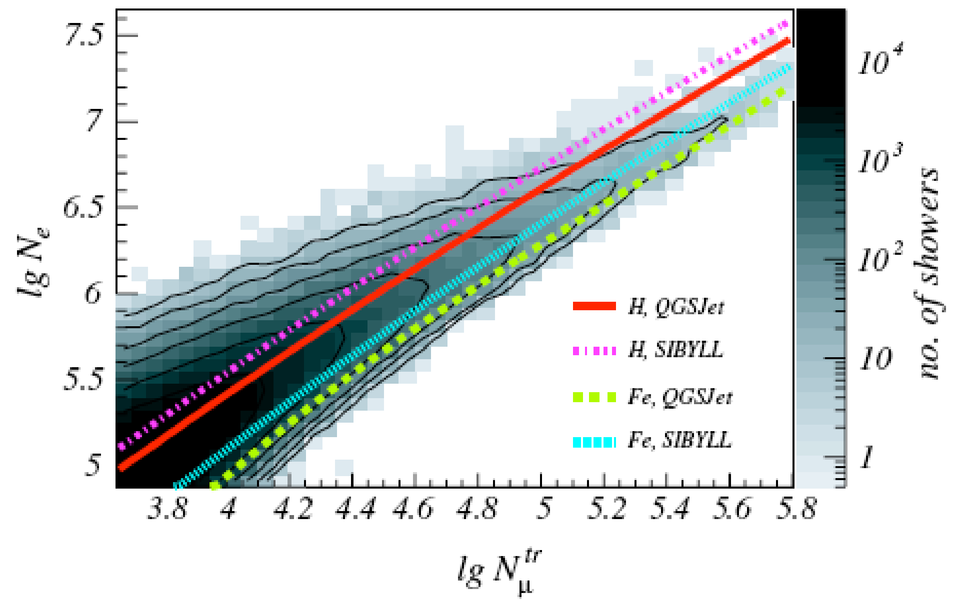

Fig. 22. Two-dimensional shower size spectrum of $\lg N_e$ and $\lg N_\mu^{tr}$ together with isolines and lines of the most probable values for proton and iron induced showers for both simulations.

Polygonato vs KASCADE

>25%

Table B.1
Differential flux values of the all particle energy spectrum for QGSJet 01 and SIBYLL 2.1 based analysis

Energy [GeV]	$dJ/dE \pm$ stat. $\pm$ syst. (QGSJet) [$m^{-2}\,s^{-1}\,sr^{-1}\,GeV^{-1}$]	Horandel APP19(2003)193	$dJ/dE \pm$ stat. $\pm$ syst. (SIBYLL) [$m^{-2}\,s^{-1}sr^{-1}\,GeV^{-1}$]
1.78×10^6	$(6.54 \pm 0.25 \pm 2.20) \times 10^{-13}$	4,75E-13	$(6.33 \pm 0.21 \pm 1.31) \times 10^{-13}$
2.24×10^6	$(3.54 \pm 0.13 \pm 0.75) \times 10^{-13}$	2,51E-13	$(3.45 \pm 0.14 \pm 0.70) \times 10^{-13}$
2.82×10^6	$(1.80 \pm 0.08 \pm 0.49) \times 10^{-13}$	1,31E-13	$(1.80 \pm 0.09 \pm 0.38) \times 10^{-13}$
3.55×10^6	$(1.01 \pm 0.05 \pm 0.22) \times 10^{-13}$	6,79E-14	$(1.00 \pm 0.05 \pm 0.22) \times 10^{-13}$
4.47×10^6	$(4.90 \pm 0.27 \pm 1.00) \times 10^{-14}$	3,47E-14	$(4.91 \pm 0.27 \pm 1.02) \times 10^{-14}$
5.62×10^6	$(2.59 \pm 0.18 \pm 0.56) \times 10^{-14}$	1,76E-14	$(2.62 \pm 0.14 \pm 0.55) \times 10^{-14}$
7.08×10^6	$(1.20 \pm 0.11 \pm 0.26) \times 10^{-14}$	8,80E-15	$(1.36 \pm 0.10 \pm 0.28) \times 10^{-14}$
8.91×10^6	$(6.41 \pm 0.62 \pm 1.35) \times 10^{-15}$	4,39E-15	$(6.26 \pm 0.46 \pm 1.30) \times 10^{-15}$
1.12×10^7	$(2.81 \pm 0.35 \pm 0.59) \times 10^{-15}$	2,19E-15	$(3.63 \pm 0.28 \pm 0.75) \times 10^{-15}$
1.41×10^7	$(1.54 \pm 0.22 \pm 0.33) \times 10^{-15}$	1,08E-15	$(1.48 \pm 0.14 \pm 0.31) \times 10^{-15}$
1.78×10^7	$(6.24 \pm 1.35 \pm 1.39) \times 10^{-16}$	5,33E-16	$(7.57 \pm 0.78 \pm 0.16) \times 10^{-16}$
2.24×10^7	$(3.09 \pm 0.78 \pm 0.64) \times 10^{-16}$	2,65E-16	$(4.05 \pm 0.51 \pm 0.87) \times 10^{-16}$
2.82×10^7	$(1.98 \pm 0.45 \pm 0.43) \times 10^{-16}$	1,31E-16	$(1.87 \pm 0.23 \pm 0.44) \times 10^{-16}$
3.55×10^7	$(8.10 \pm 2.52 \pm 1.93) \times 10^{-17}$	6,42E-17	$(8.81 \pm 0.14 \pm 2.38) \times 10^{-17}$
4.47×10^7	$(4.22 \pm 1.16 \pm 1.14) \times 10^{-17}$	3,10E-17	$(3.65 \pm 0.66 \pm 1.18) \times 10^{-17}$
5.62×10^7	$(1.83 \pm 0.74 \pm 0.79) \times 10^{-17}$	1,48E-17	$(2.29 \pm 0.45 \pm 0.89) \times 10^{-17}$
7.08×10^7	$(1.37 \pm 0.40 \pm 0.53) \times 10^{-17}$	6,81E-18	$(9.29 \pm 2.72 \pm 5.38) \times 10^{-18}$
8.91×10^7	$(6.07 \pm 2.87 \pm 4.02) \times 10^{-18}$	3,05E-18	$(5.81 \pm 2.07 \pm 4.31) \times 10^{-18}$

The first column of errors denotes the statistical uncertainty, the second column the systematic uncertainty.

Measurements that have impact on (or are affected by) CR composition and Interaction models

- Unprecedented statistics of Atmospheric Muons

  MACRO ~0.1 Hz (3150 mwe min depth)

  AMANDA-II ~80 Hz rate (19 strings in 1500-2500 mwe depth)

  First IceCube run rates: 4500 Hz in 22 strings

  Text

  1.5 kHz full array (1450-2450 mwe depth)
- Unprecedented statistics of Atmospheric Neutrinos

  MACRO @ Gran Sasso 150/yr (76 x 12 x 9 m^3)

  AMANDA-II ~2.7/d

  IceCube 9 strings ~1.7/d

  IceCube 80 strings ~140/d

The high potential of high muon statistics

We have sensitivity to hadronic models already in AMANDA-II

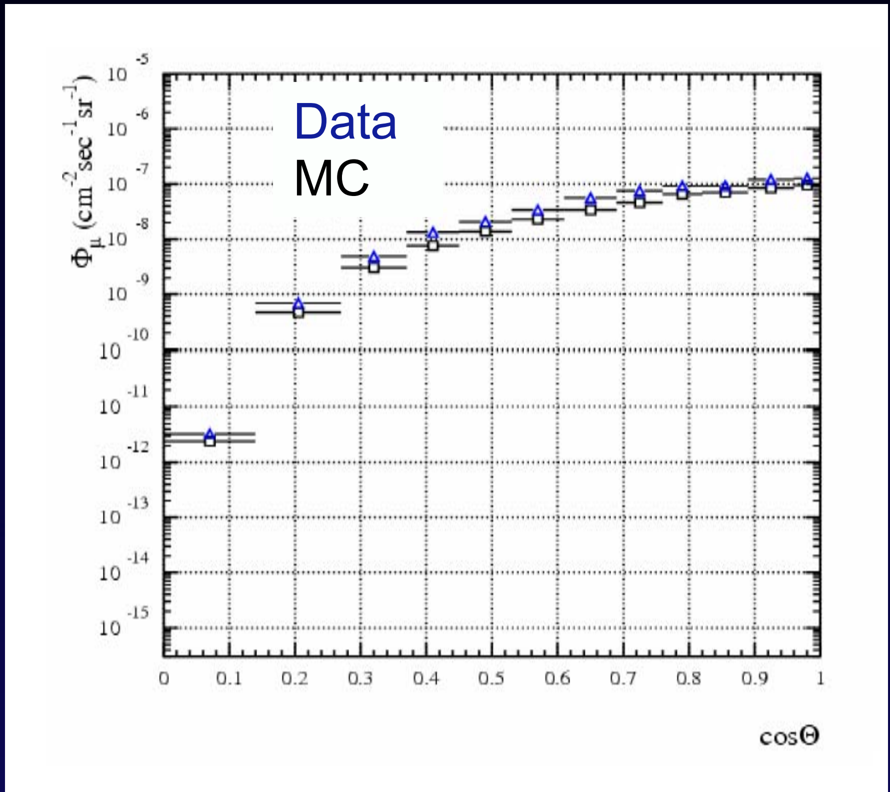

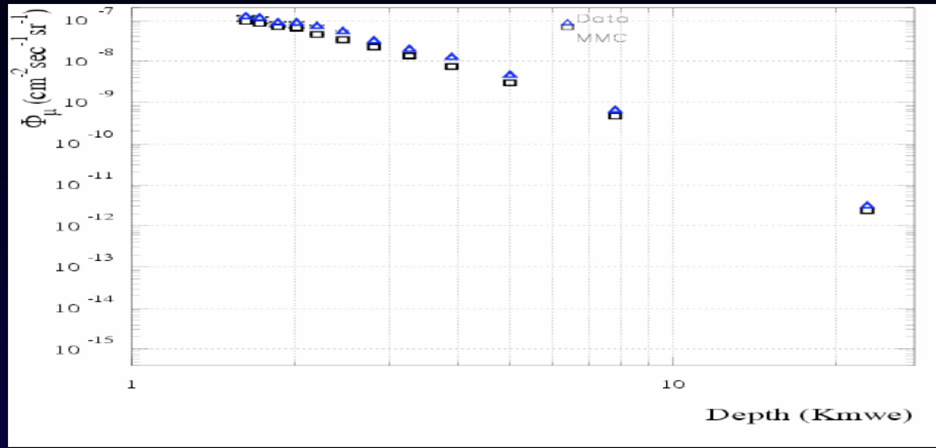

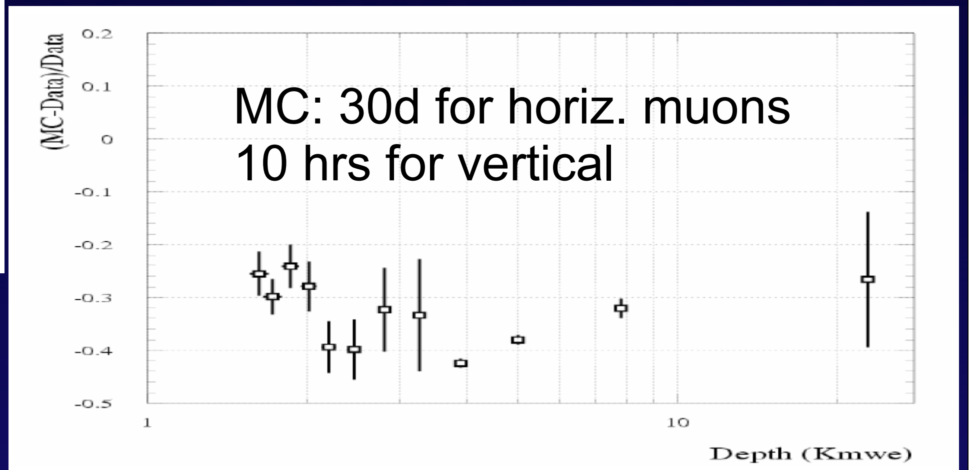

Preliminary 30 d in 2001 data presented at TeV ParticleAstrophysics II

Muons<2TeV L3+C data compared to interaction models

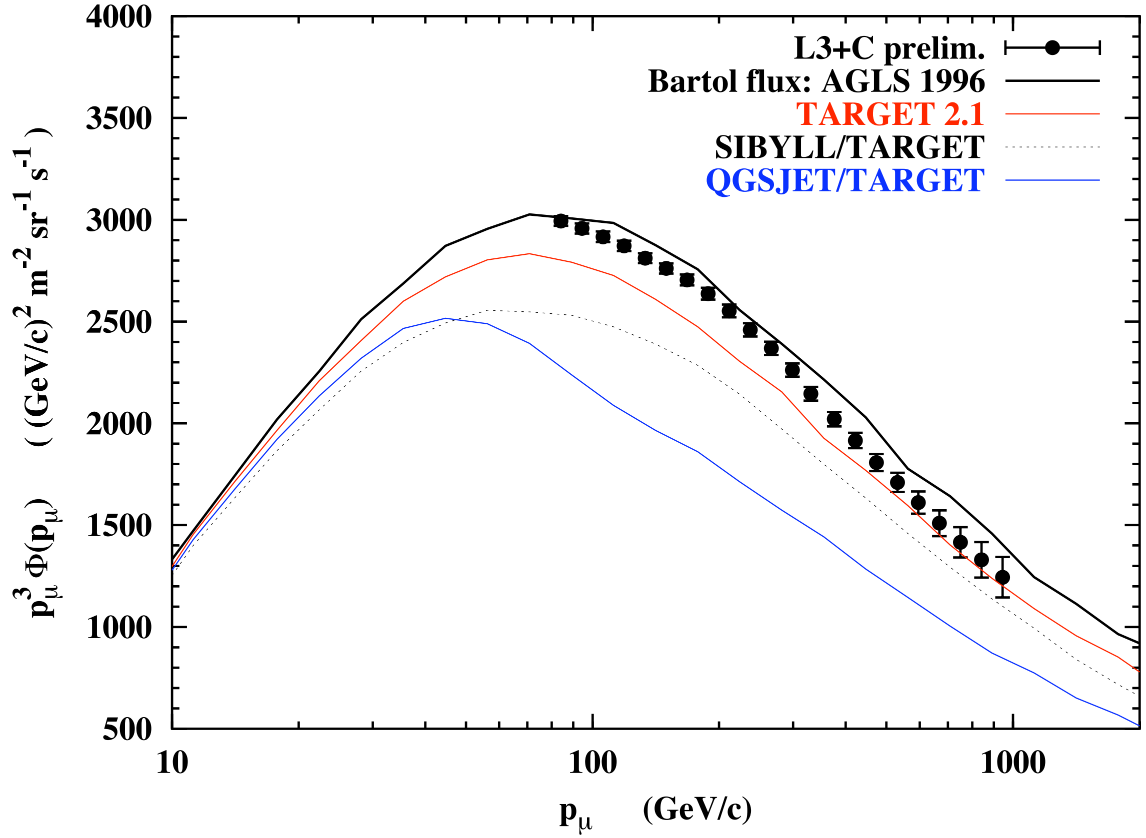

Plot by R. Engel

QGSJet01 could produce too few muons at AMANDA-II depth

MEAN #μS AT GROUND

- R. Engel at al, Aspen 2007

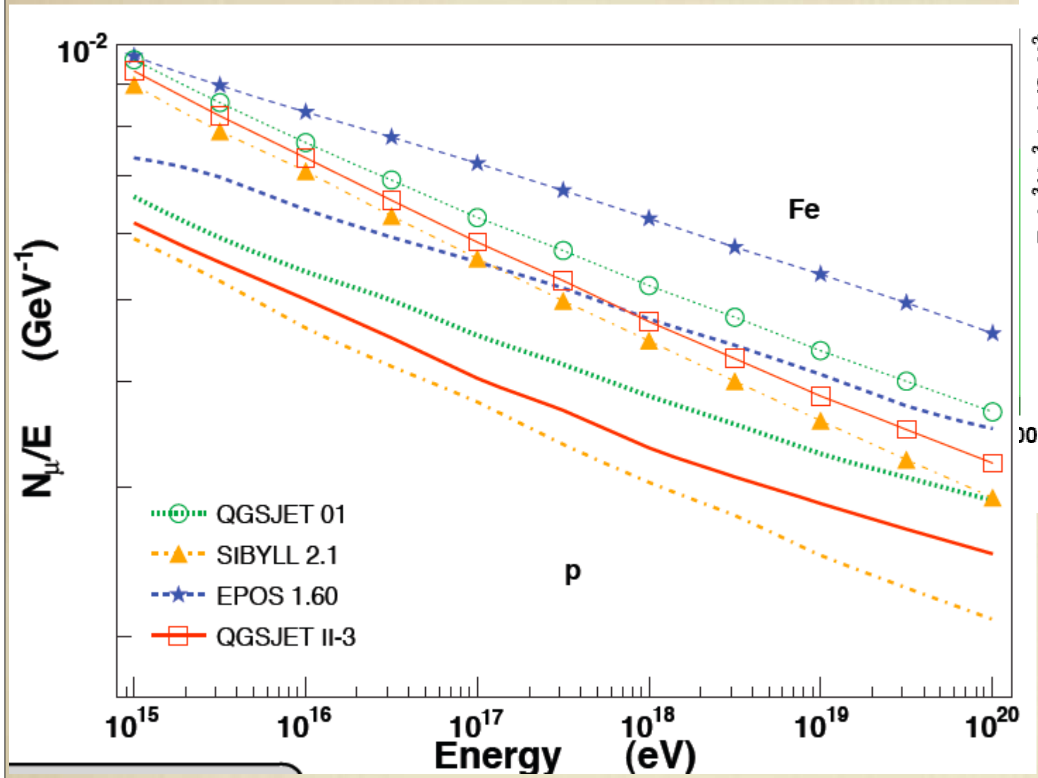

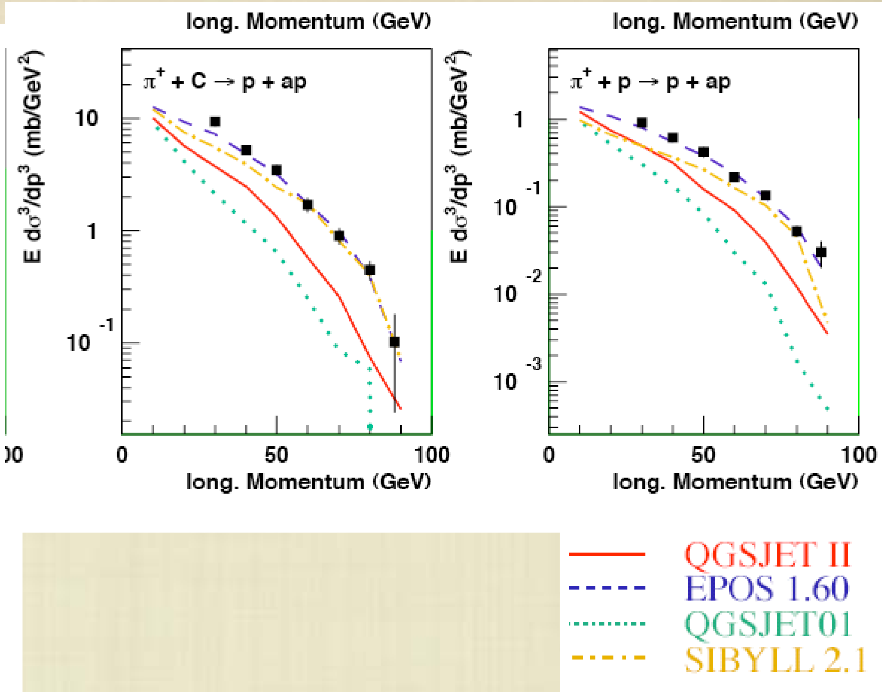

EPOS predicts up to 5 times more baryons in hadronic shower core at high energy

Iron (QGSJET) = proton (EPOS)

(at 10^{18} eV)

EPOS, astro-ph/0611311

EPOS: much flatter lateral distribution for both muons and em. particles

To produce such a high muon multiplicity EPOS needs a pion-air multiplicity a factor of 2 higher than QGSJET-02

EPOS

- TO PRODUCE SUCH A HIGH MUON MULTIPLICITY EPOS NEEDS A PION-AIR MULTIPLICITY A FACTOR OF 2 HIGHER THAN QGSJET-02

EPOS predicts up to 5 times more baryons in hadronic shower core at high energy

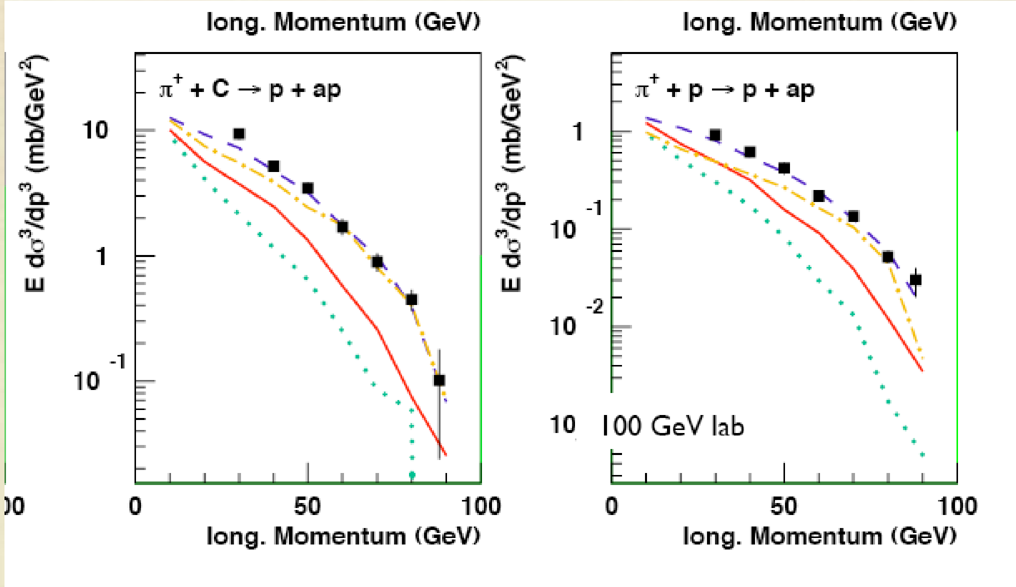

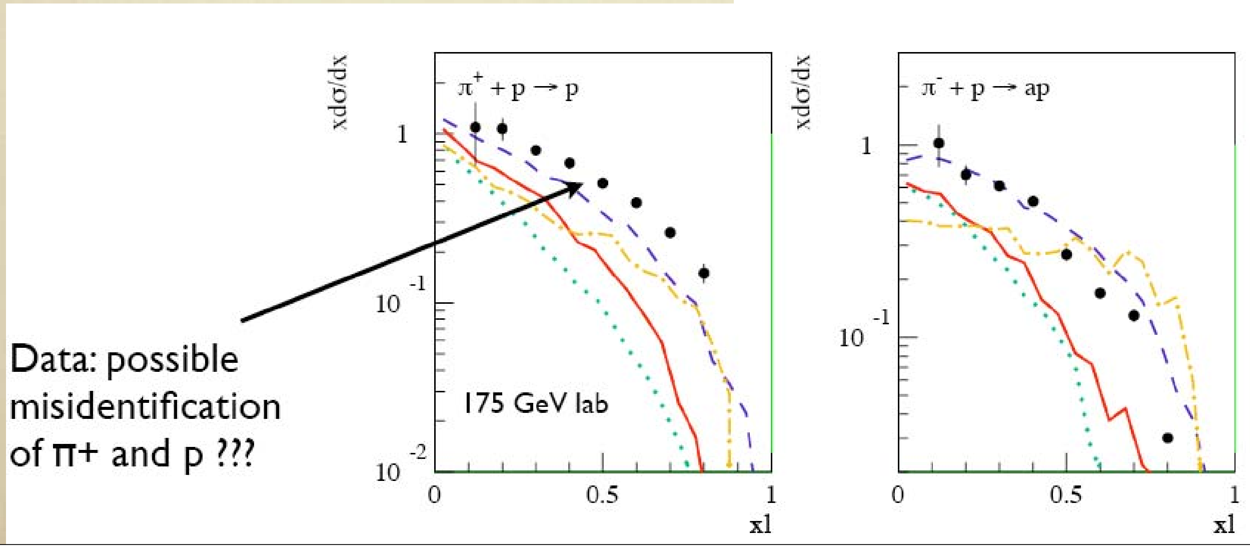

Atmospheric Neutrinos

- Conventional flux references:

Bartol group: Barr, Gaisser, Lipari, Stanev, Robbins, tables in http://www-pnp.physics.ox.ac.uk/~barr/fluxfiles/0408i/index.html, PRD70 (2004) 023006 and PRD74 (2006) 094009.

HKKM: Honda, Kajita, Kasahara, Midorikawa, PRD70 (2004) 043008 and PRD75 (2007) 043006, http://www.icrr.u-tokyo.ac.jp/~mhonda/

FLUKA: Battistoni, Ferrari, TM, Sala, Astrop. Phys. 19 (2003) 269 and hep-ex/0305208 high energy at ICRC2003

Prompt fluxes:

Naumov et al. (RQPM), Phys. Lett. B510 (2001)173
Martin et al (pQCD), Acta Phys.Polon. B34 (2003) 3273
Costa, Astropart. Phys. 16 (2001) 193
Zas et al, Astrop Phys 1 (1993) 297

One difficulty

- traditionally atmospheric neutrino calculations are different than what is used to simulate atmospheric muons
- Muons are simulated using CORSIKA and different CR composition
- Neutrinos are simulated using weighting techniques, so $E^{-\gamma}$ fluxes are weighted for values of fluxes from HKKM, Bartol, FLUKA and other prompt models
- We often use the ‘inverted-analysis’ to check our neutrino measurement on the high statistics of atmospheric muons

Diffuse Flux World-Wide Results on diffuse neutrino fluxes

AMANDA-II limit (GHill et al, Neutrino2006) is a factor of 4 from W&B
IceCube will be able to investigate the region were neutrinos should exist

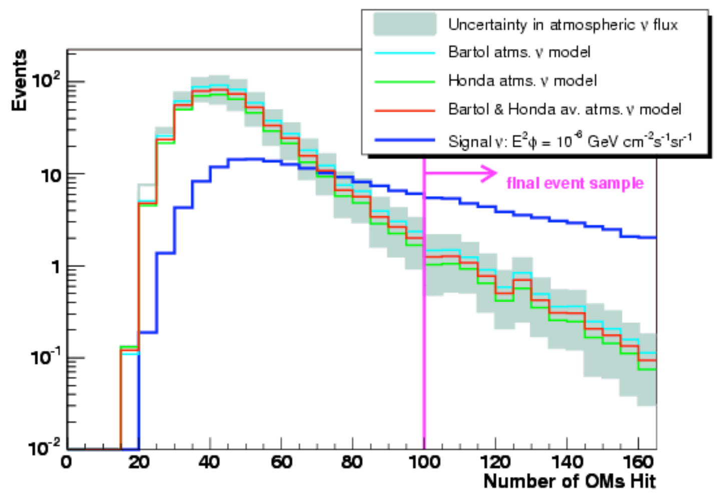

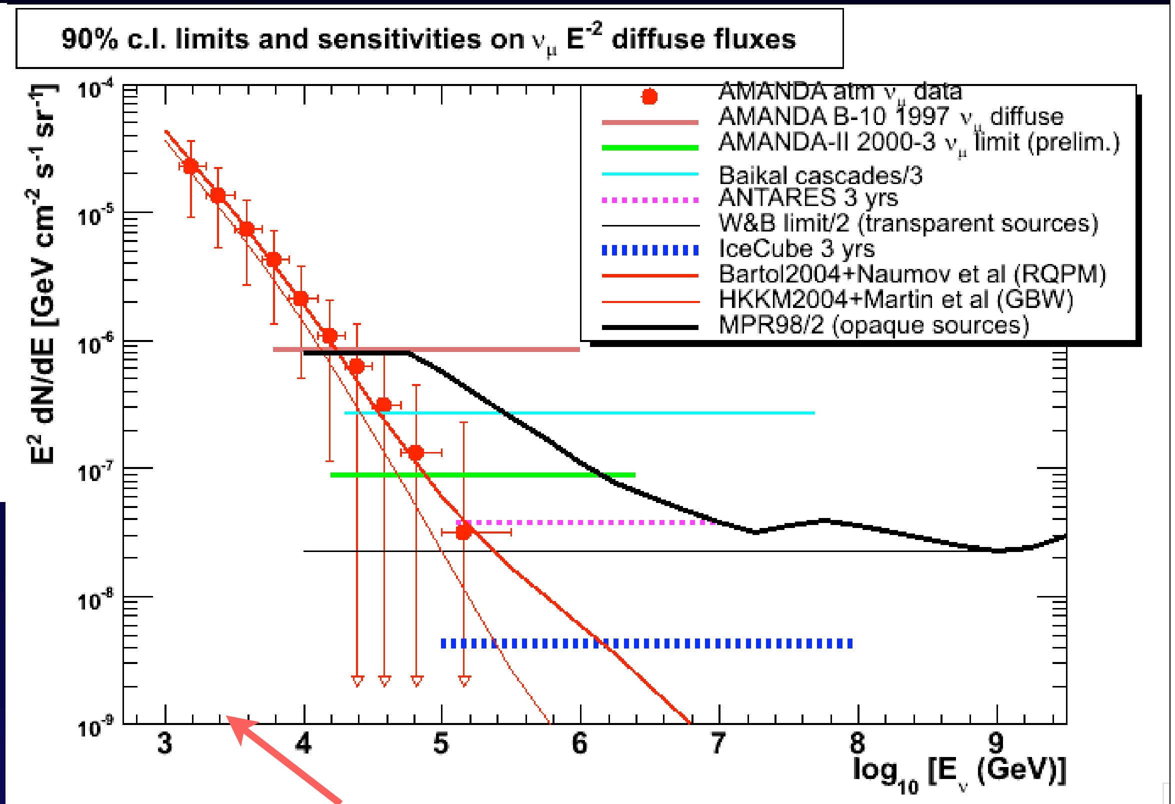

AMANDA-II atm ν spectrum ICRC2005

The high energy region of atm neutrino spectra requires good knowledge. It is a S and B for NTs.

Conventional neutrinos

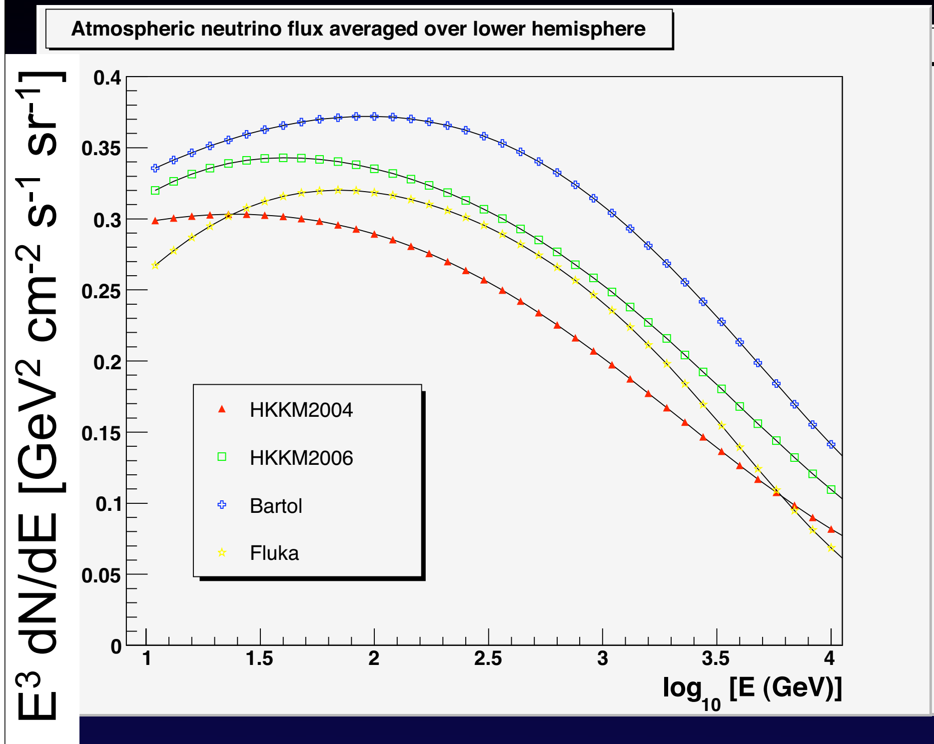

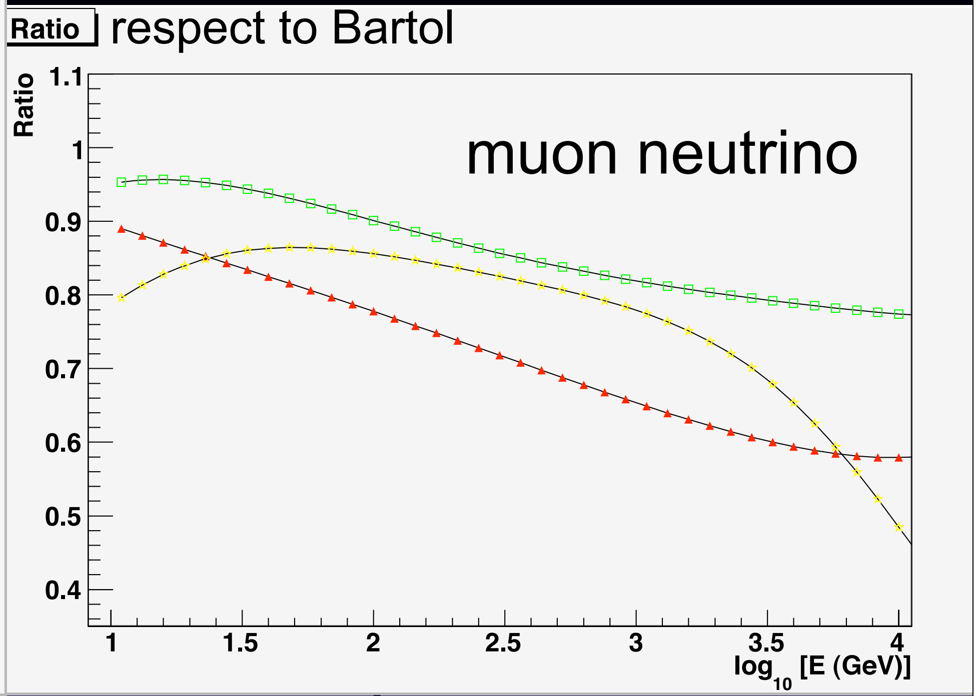

HKKM2006 improves much compared to HKKM2004 and closer to FLUKA and Bartol thanks to benchmark on muns in the atmosphere.
Uncertainties around 10TeV remain high
(smaller for muon neutrino+antineutrino since Bartol neutrino>HKKM2006 but antineutrino Bartol<HKKM2006)

Charm muons and neutrinos: signal and background

Prompt muons/neutrinos have flatter spectra (prompt decay keeps CR primary shape) and flatter angular distribution (short decay length)
Muon lateral distribution may keep track of larger p_T in coincident IceTop-IceCube events for E_μ >10-100 TeV events but effects of showers tend to wash out this signature.

WE NEED A FULL SIMULATION OF SHOWERS INCLUDING CHARM

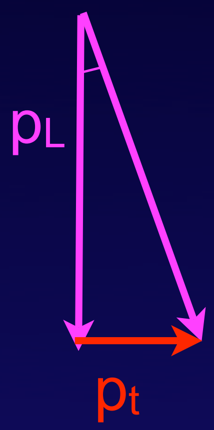

$$d = \frac{h p_T}{E_\mu}$$

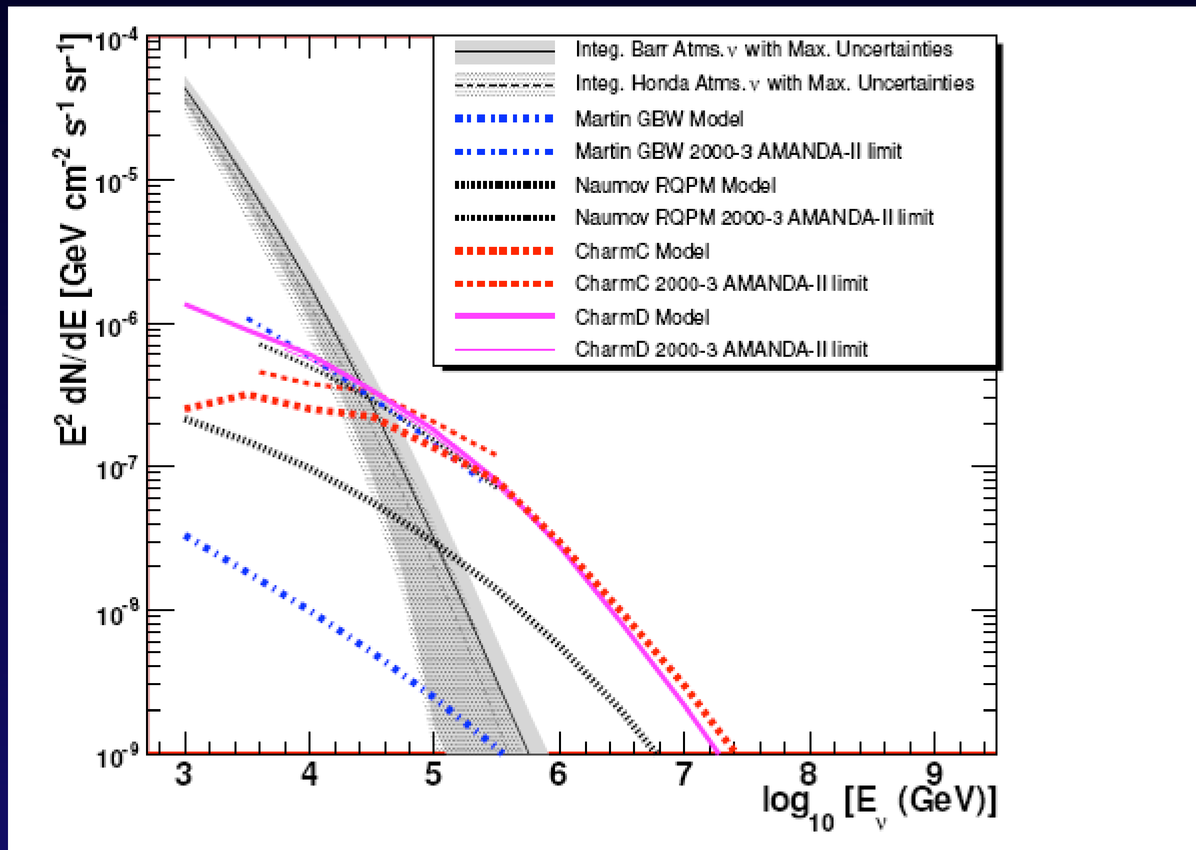

P_T from Corsika-DPMJET II.55

monoenergetic interactions of protons on Nitrogen

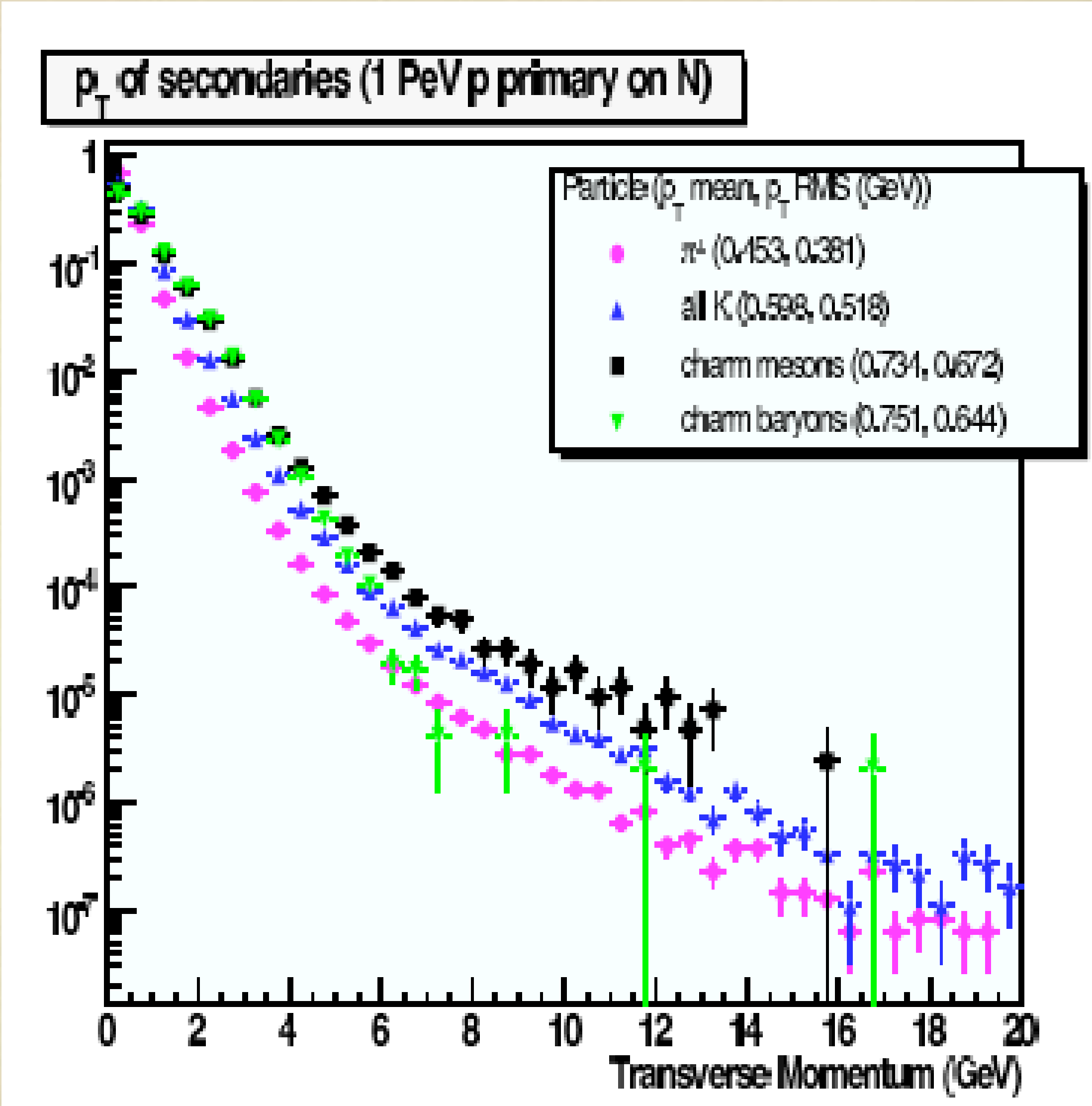

CORSIKA 6321 +DPMJETII.55 where charm is allowed to decay (Heck+A. Meli)

Lateral muon DR

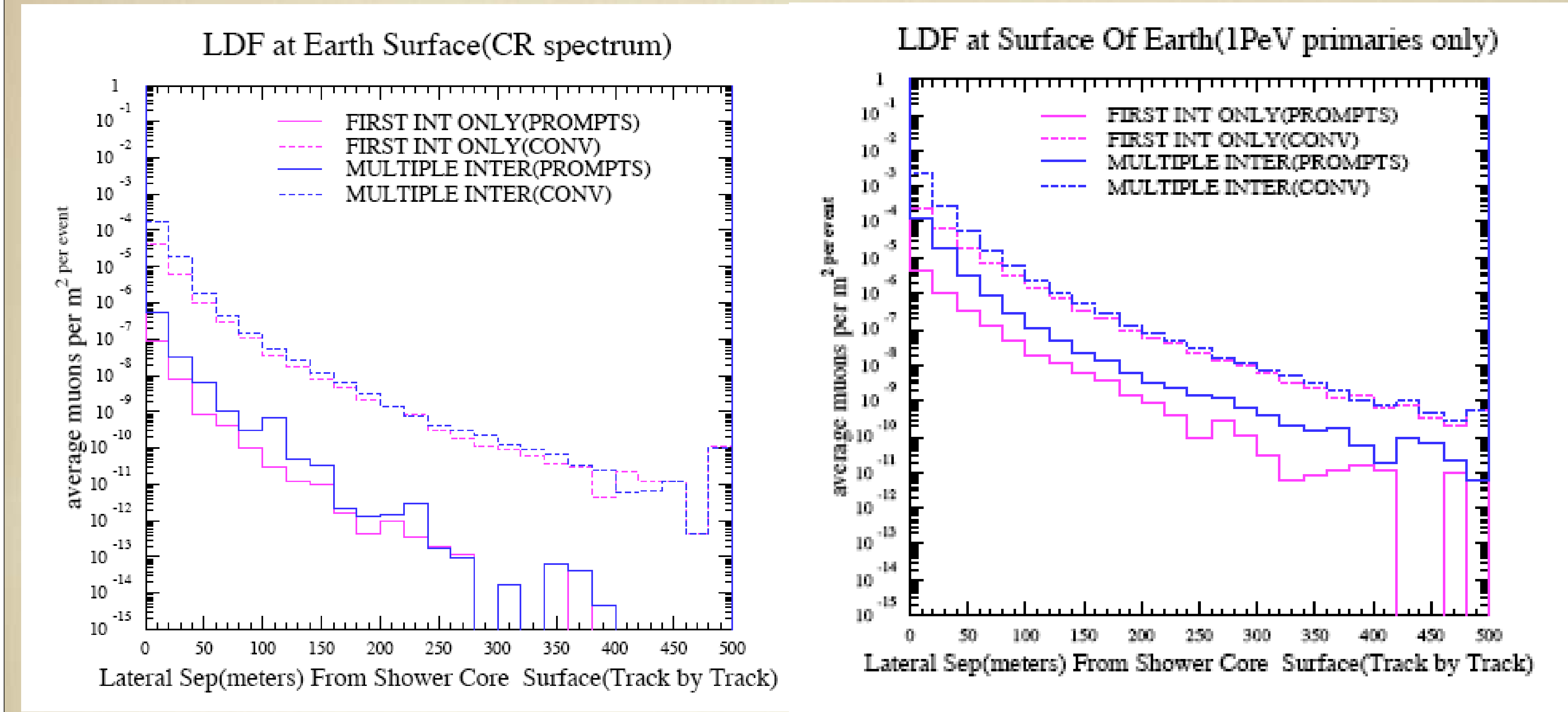

PROMPT = ALL MUONS IN EVENTS WITH CHARM

THIS FIRST RESULT NEEDS TO BE CONFIRMED

Charm predictions

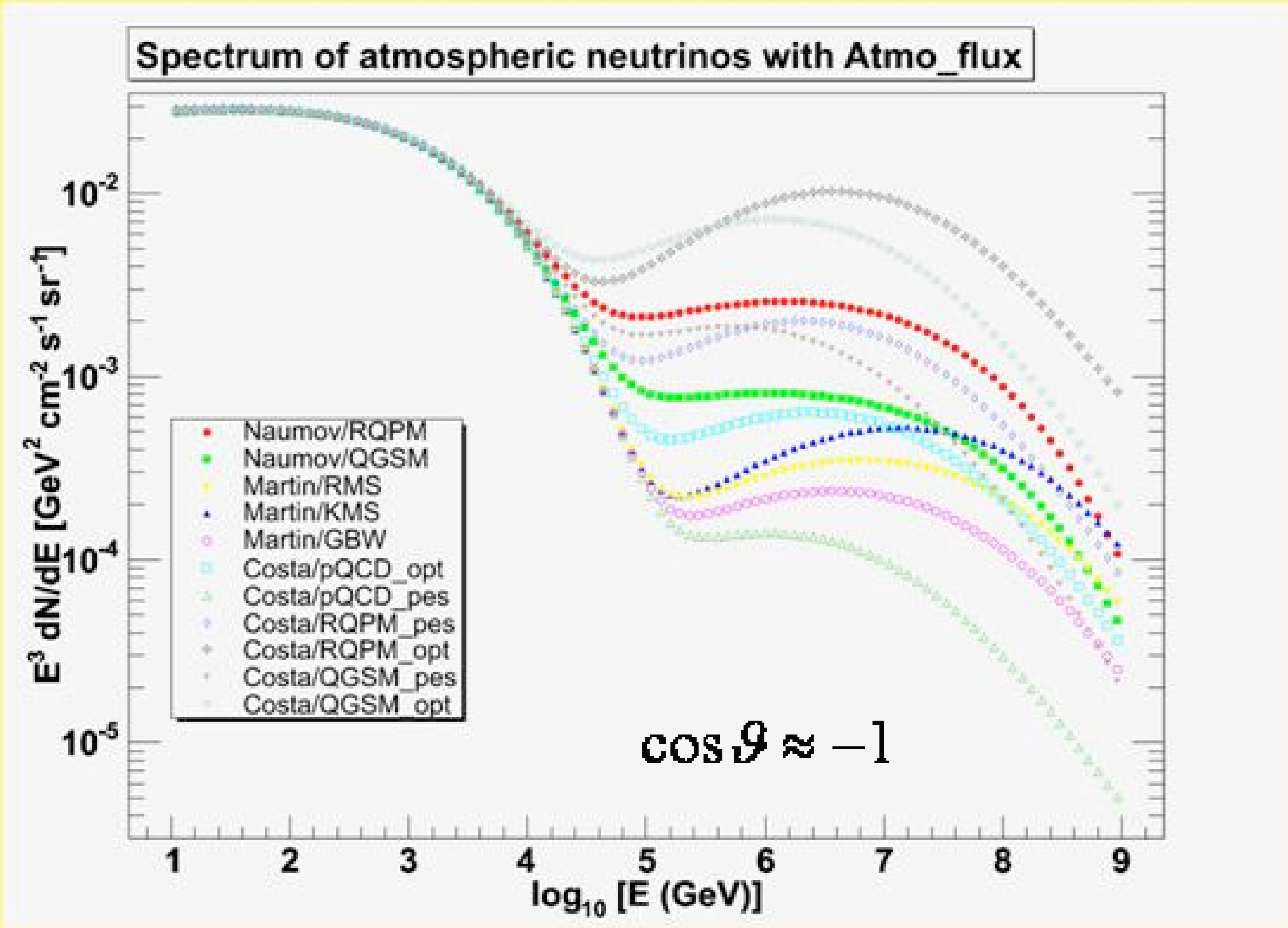

Hadronic Models

- Main challenge: description of transition region between soft and semi-hard (pQCD is applicable) processes

- DPMJET and QGSJET based on Regge-Gribov theory of multi-pomeron exchange
  DPMJET-III includes lowest order diagrams of pomeron-pomeron interactions)
  QGSJET: hadronic multiple scattering as multiple exchanges of Pomerons (corresponding to independent microscopic parton cascades). QGSJET-II treats non-linear parton effects.

- SIBYLL2.1: pomeron formalism for soft processes +semi-hard uses minijet production (similar to semi-hard pomeron scheme). uses glauber for h-N interactions. Predicts precise Feynmann scaling supported by inclusive μ measurements whereas QGSJET shows noticeable scaling violations

- EPOS employs soft and semi-hard pomeron description BUT takes into account energy-momentum correlations between multiple rescatterings. Describes non-linear pomeron-pomeron interaction graphs with parameters adjusted with RICH data.

UHE and CHARM

- to compare hadronic models at UHE we simulated monoenergetic interactions on protons on Nitrogen
- CORSIKA 6321/6600+DPMJETII.55 (Heck+A. Meli, NOT OFFICIAL): Changed treatment of heavy mesons in corsika and Charmed particles are allowed to decay immediately at interaction vertex
- FLUKA 2007+(DPMJET II.55 and DPMJET-III>100 GeV)
- we could not run DPMJET III run >1000TeV

Charged Pions at 1000TeV

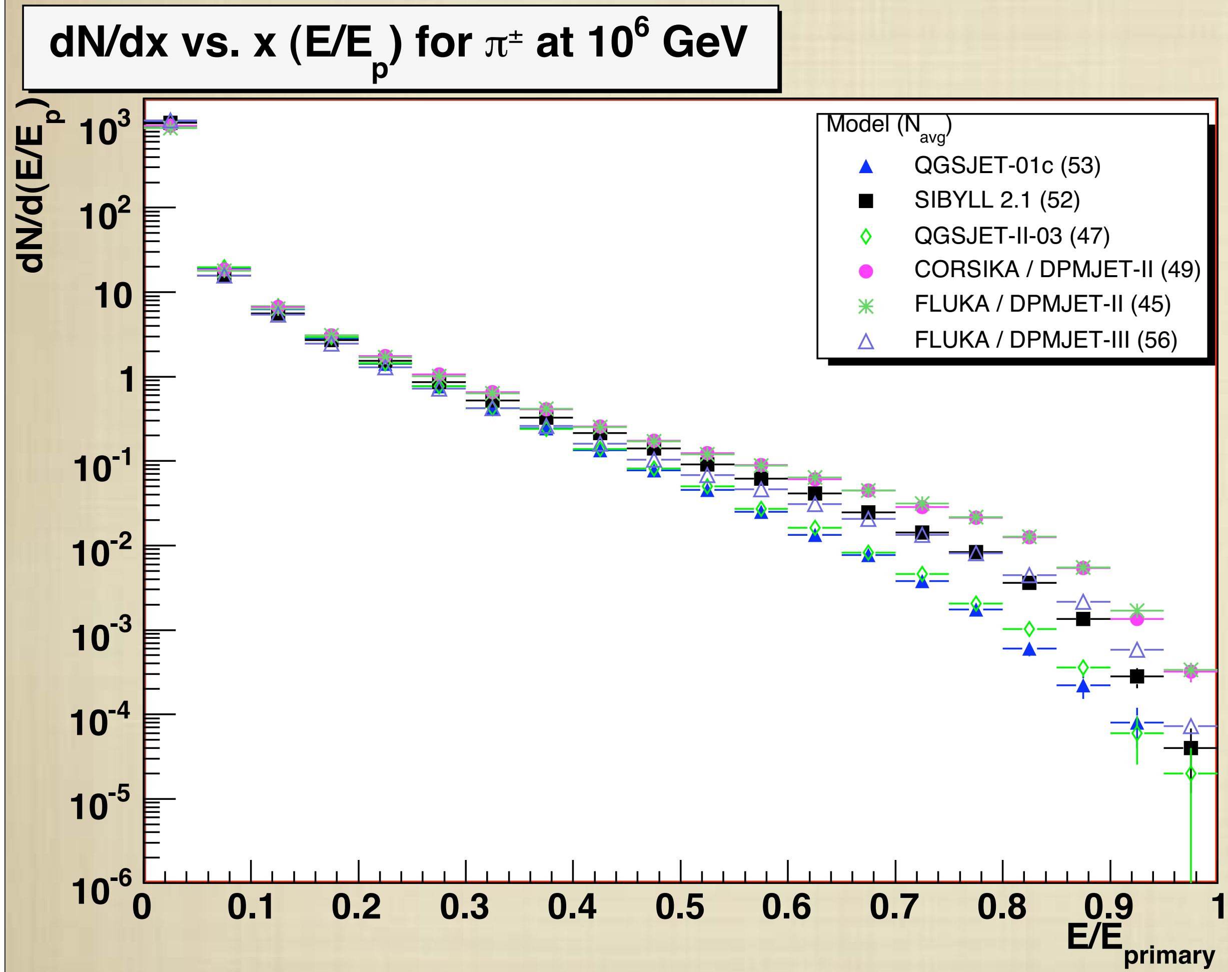

FLUKA DPMJET II and CORSIKA DPMJET II very similar and harder than all others

DPMJET III closer to SIBILL

QJSGET02 and 01 lower

Charged Kaons:

disagreement at low secondary energy
and DPMJET II in CORSIKA and FLUKA differ
No explanation for this yet

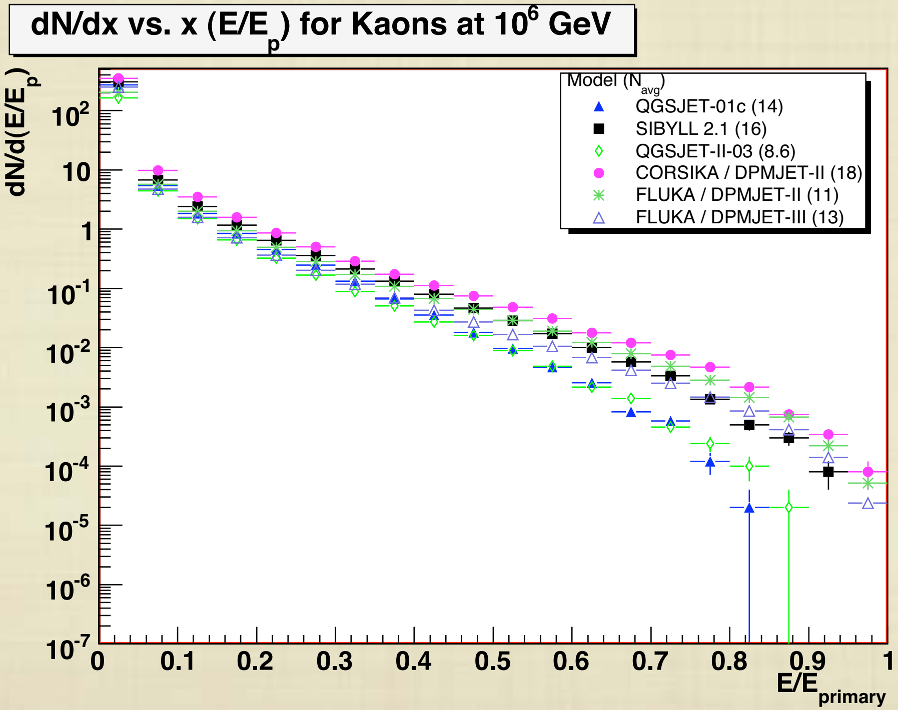

CHARM

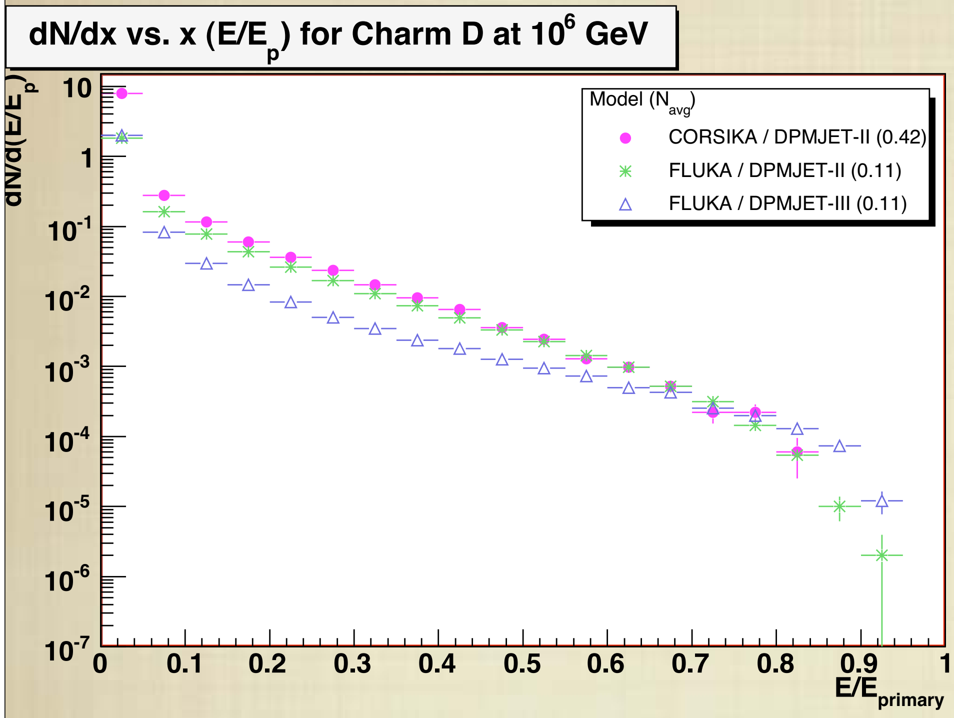

dN/dx vs. x (E/E_p) for Charm D at 10^6 GeV
Model (N_avg)
CORSIKA / DPMJET-II (0.42)
FLUKA / DPMJET-II (0.11)
FLUKA / DPMJET-III (0.11)
dN/d(E/E_p)
E/E_primary

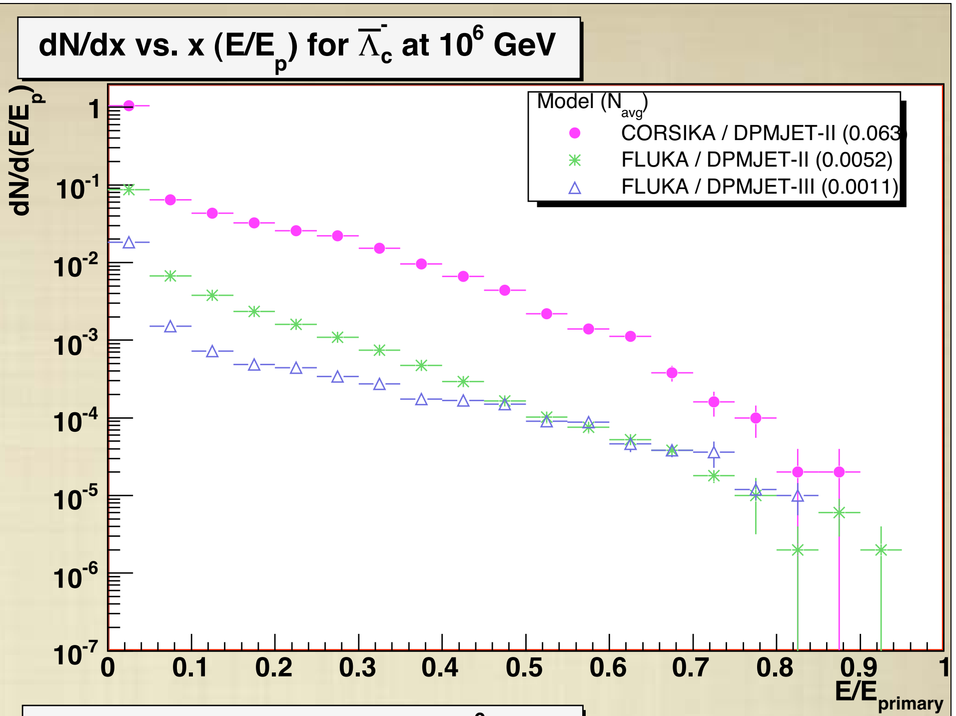

dN/dx vs. x (E/E_p) for $\overline{\Lambda}_c^-$ at 10^6 GeV
Model (N_avg)
CORSIKA / DPMJET-II (0.063
FLUKA / DPMJET-II (0.0052)
FLUKA / DPMJET-III (0.0011)
dN/d(E/E_p)
E/E_primary

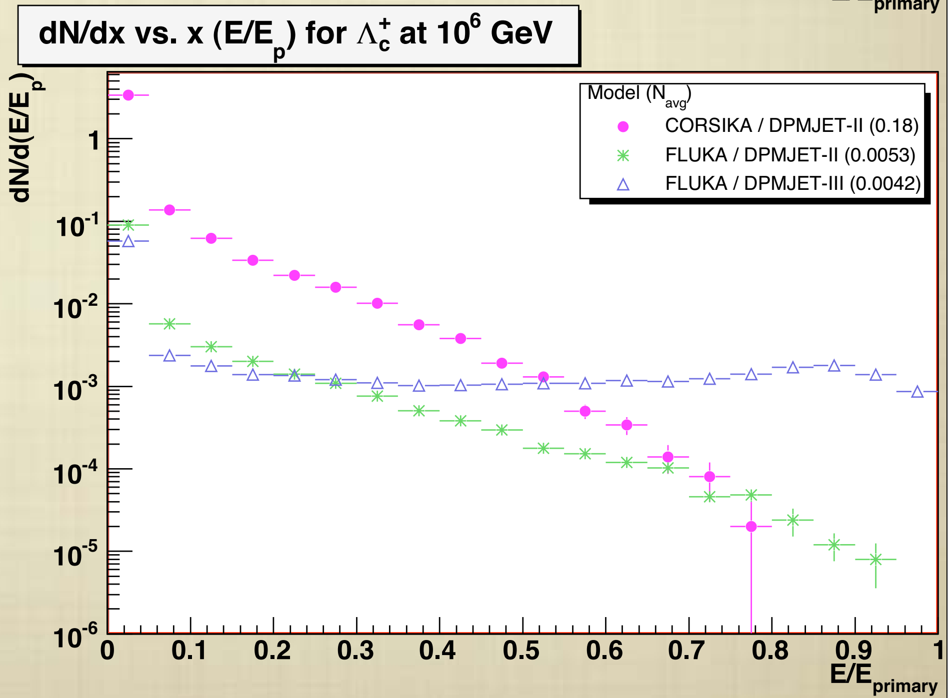

dN/dx vs. x (E/E_p) for Λ_c^+ at 10^6 GeV
Model (N_avg)
CORSIKA / DPMJET-II (0.18)
FLUKA / DPMJET-II (0.0053)
FLUKA / DPMJET-III (0.0042)
dN/d(E/E_p)
E/E_primary

P(1000TeV)+N

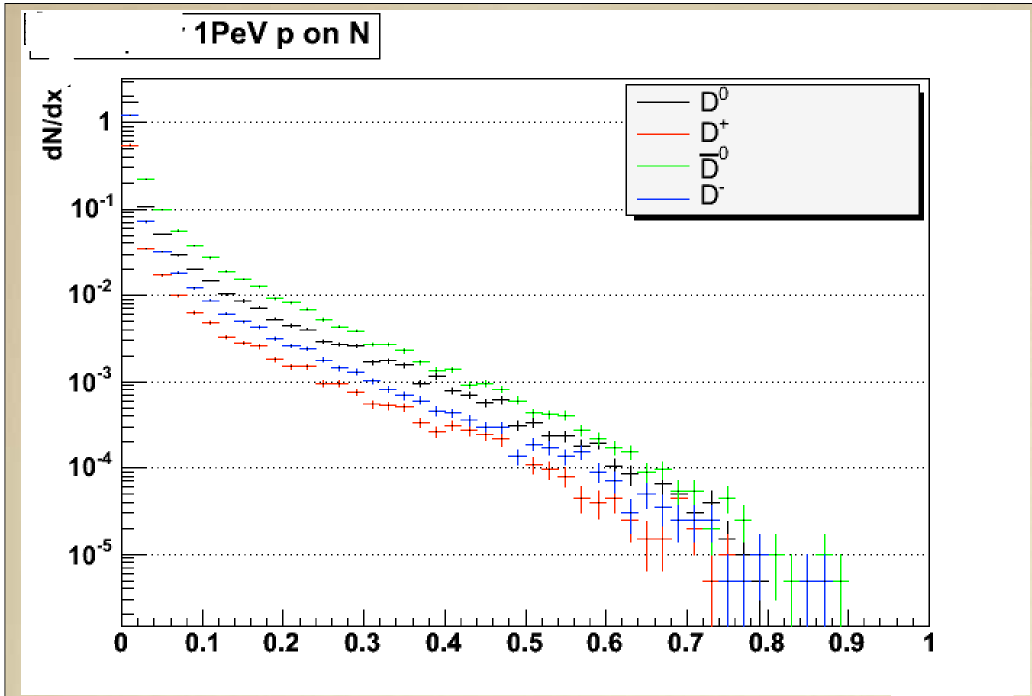

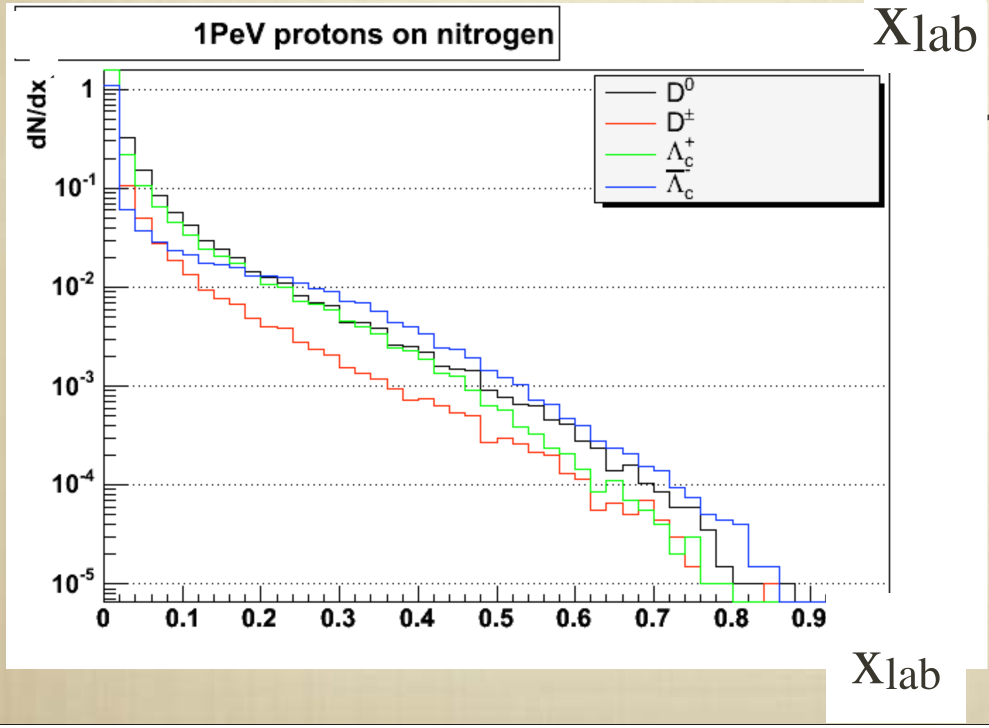

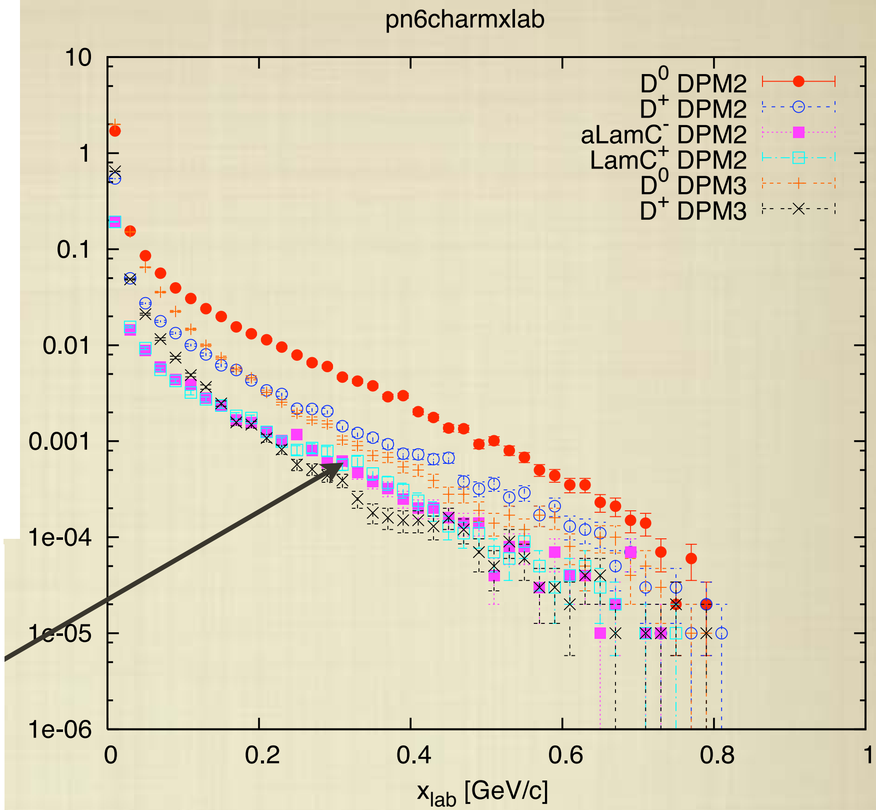

J. Ranft, DPMJETII.55 standalone

Lambdas disagree with DPMJET-II.55 in CORSIKA 6600, 1st interaction

CDF DATA: P_T IN CENTRAL REGION

P-ANTI-P AT 1.96 TEV IN CM ➜ 2 PEV LAB

abs(y) <= 1

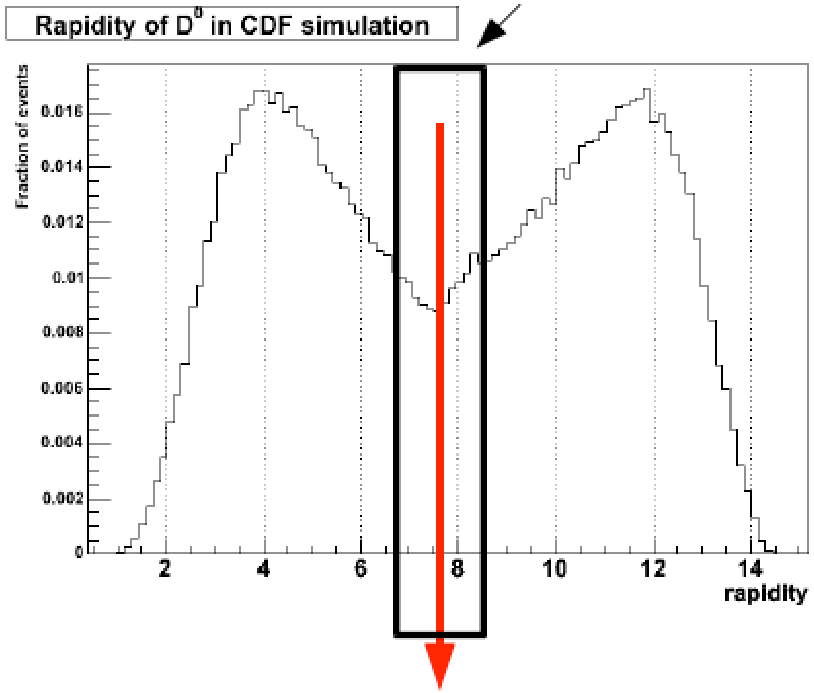

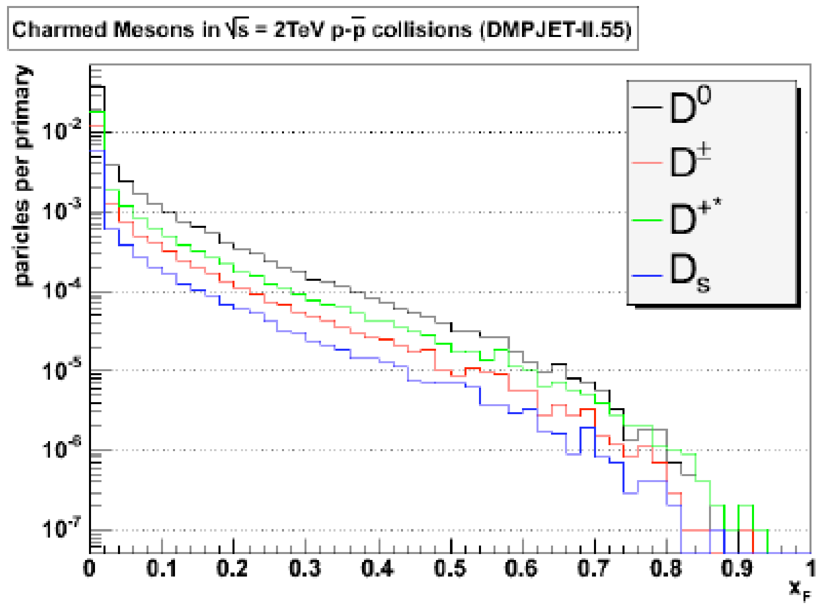

y = 0 in center-of-mass system (7.6)

$$y = \frac{1}{2}\log\frac{E + p_L}{E - p_L}$$

A Lorentz boost along the direction of the incident particle adds a constant,

$\log(\gamma + \gamma\beta)$ = log(2 x 10^3) =7.6 to the rapidity

P_T DISTRIBUTIONS

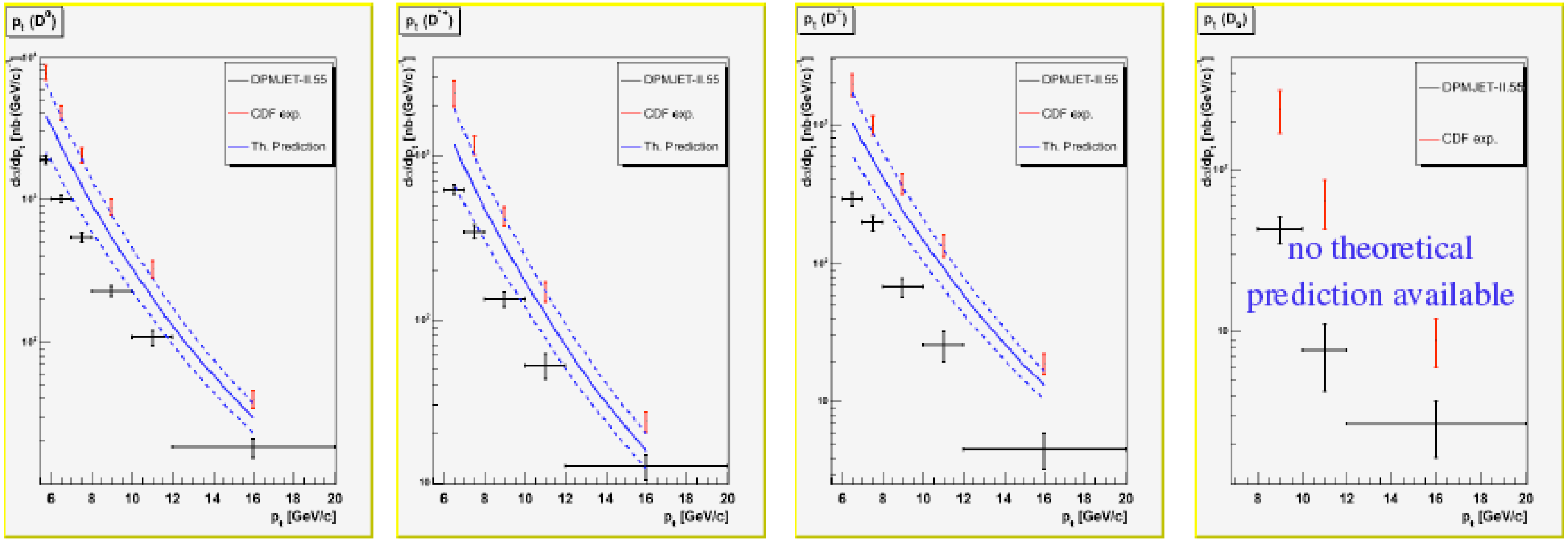

10M DPMJET proton-antiproton interactions

Data from CDF (hep-ex/0307080)

Prediction by Cacciari and Nason (hep-ph/0306212)

PHENIX (RICH)

- p+p at sqrt(s)=200 GeV
- Muon production at forward rapidity region $(1.5 \leq |\eta| \leq 1.8)$
- spectra from charm semileptonic decays in, 30 nb^{-1} integrated luminosity
- hep-ex/0609032

PHENIX at Large rapidity

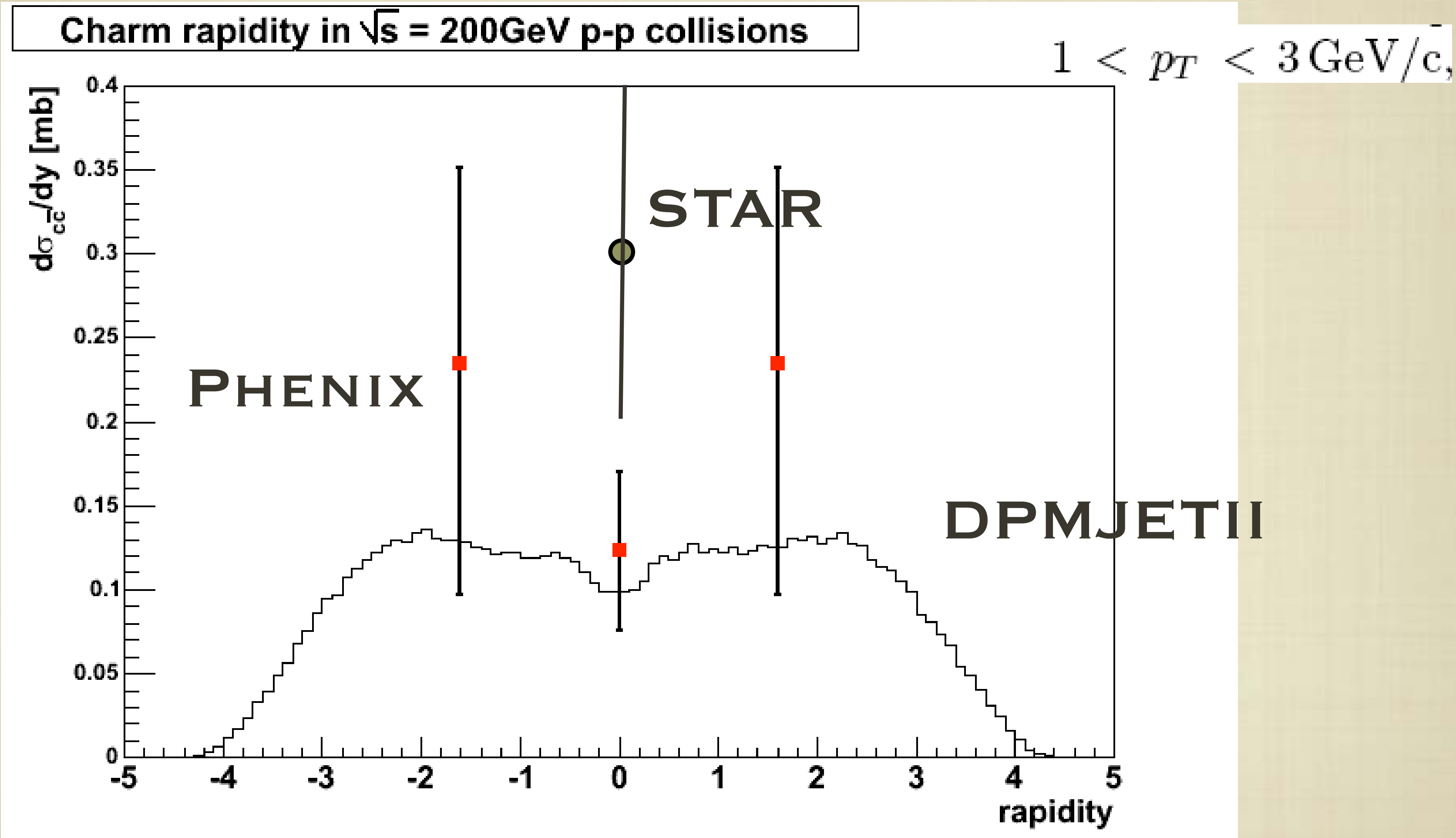

- Only charmed D and baryons

NA27 LEBC-EHS coll.

Data p(400GeV) + p
CERN/EP 88-49
Charmed mesons

$n = 4.9 \pm 0.5$

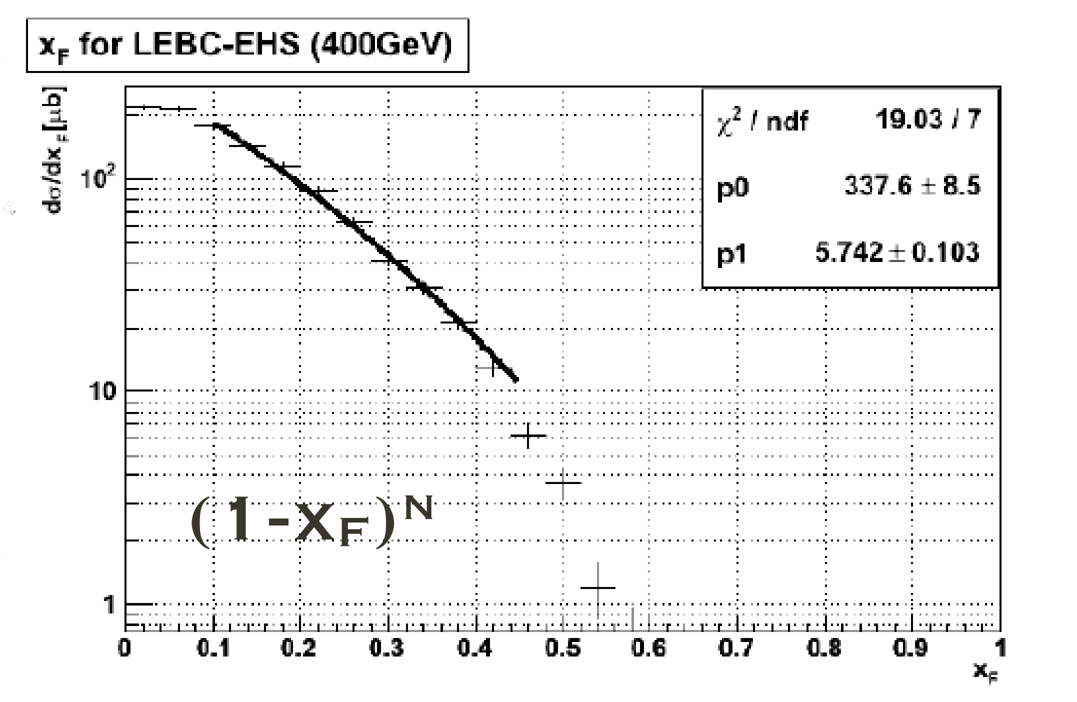

Battistoni et al.

Astropart.Phys.4:351-364,1996

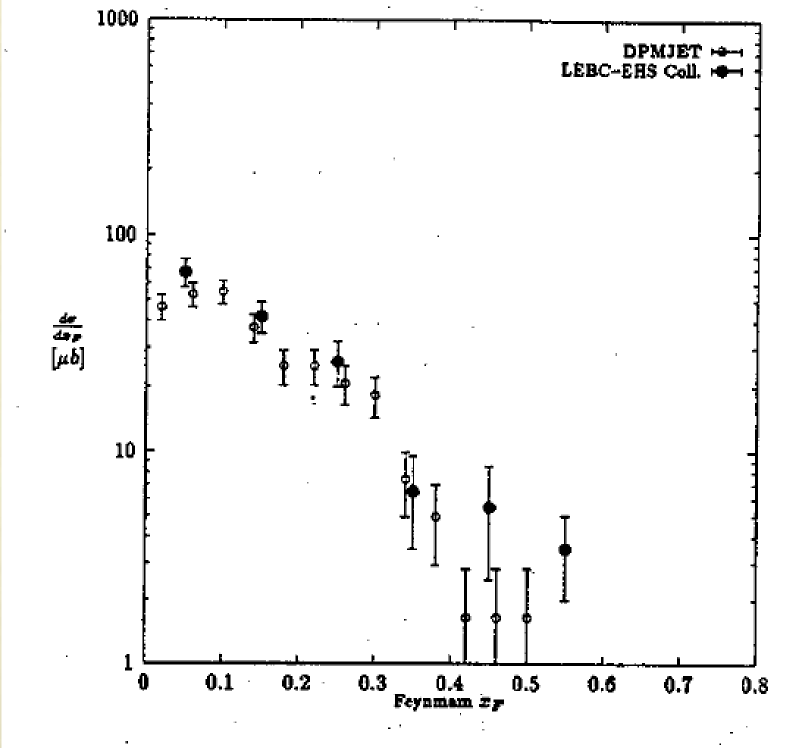

NA27 LEBC-EHS coll.

$$\frac{d^2\sigma}{dx_F\, dp_T^2} \propto (1 - |x_F|)^n\, e^{-bp_T^2}$$

Data CERN/EP 88-49

$$b = (0.99 \pm 0.09)\ (\mathrm{GeV}/c)^{-2}$$

Battistoni et al.

Astropart.Phys.4:351-364,1996

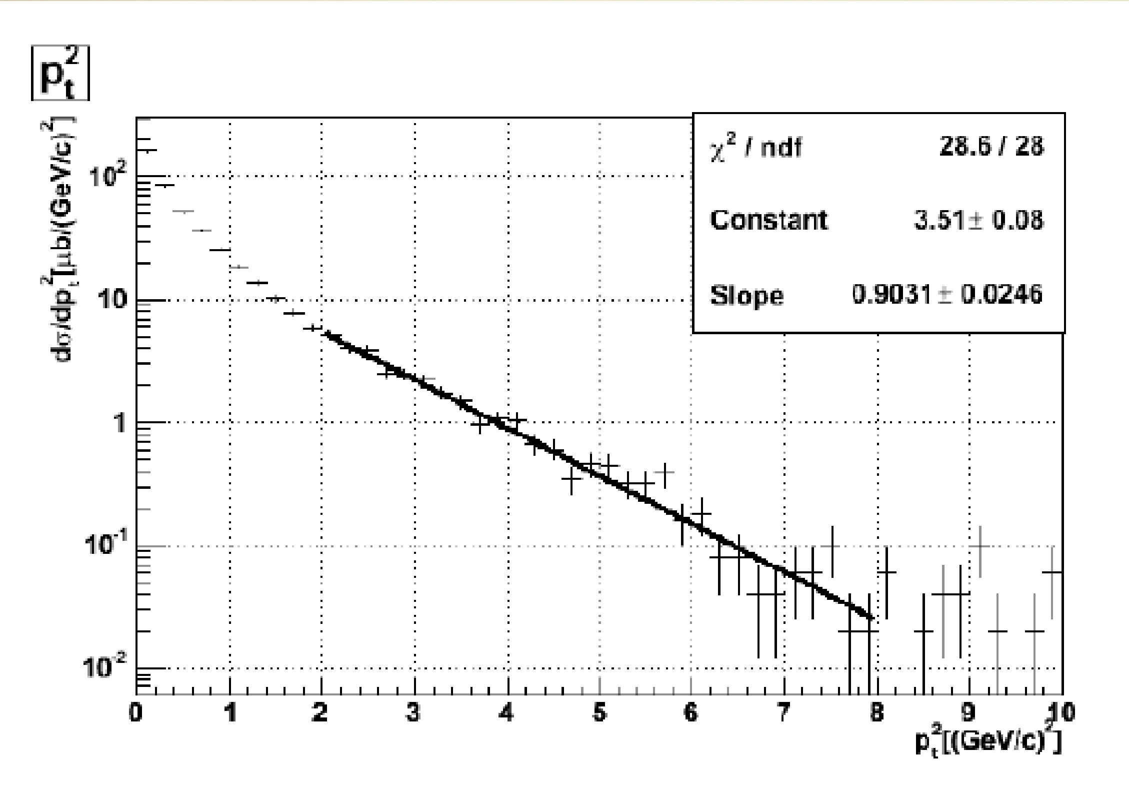

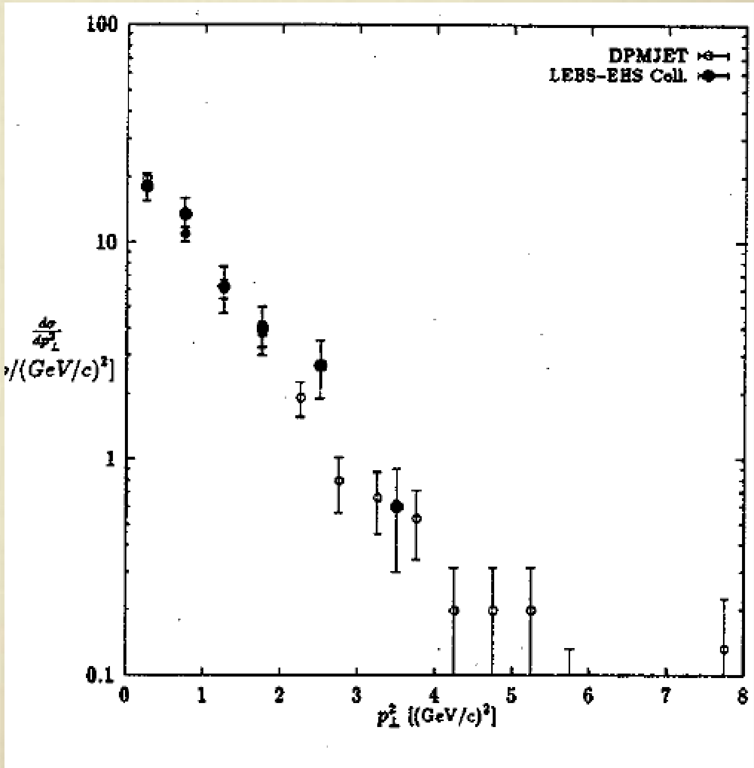

At Fermilab

$(1-|x_F|)^n e^{-ap_\perp^2}$

$n = 8.6 \pm 2.0$

Battistoni et al.

Astropart.Phys.4:351-364,1996

- PRL (1988) p(800GeV/c)+p

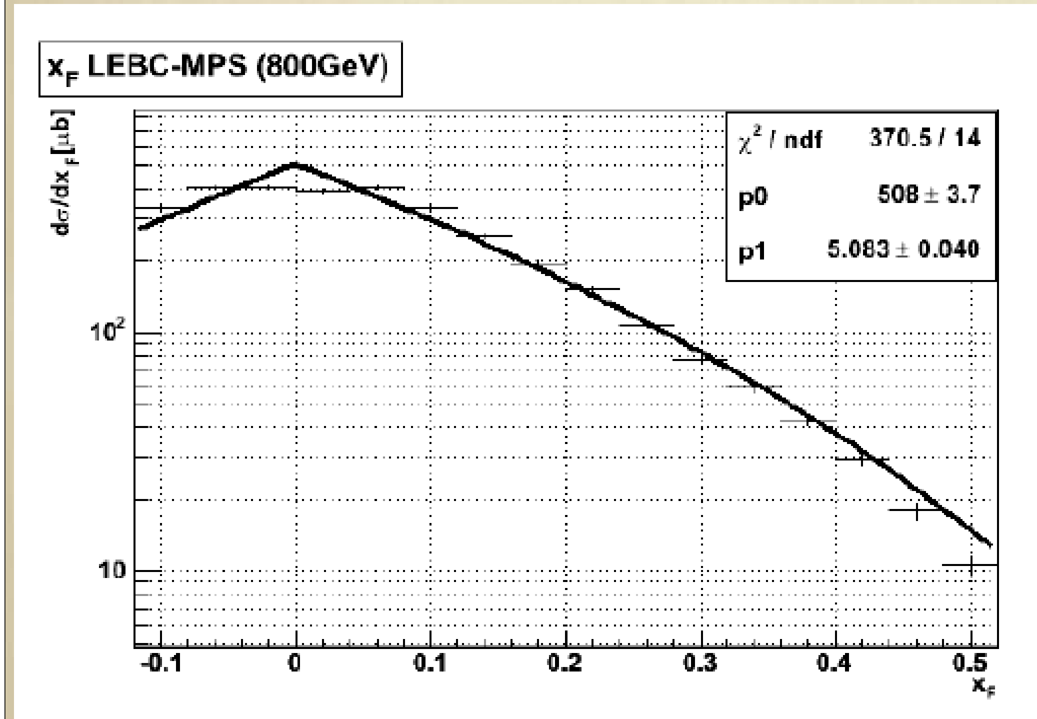

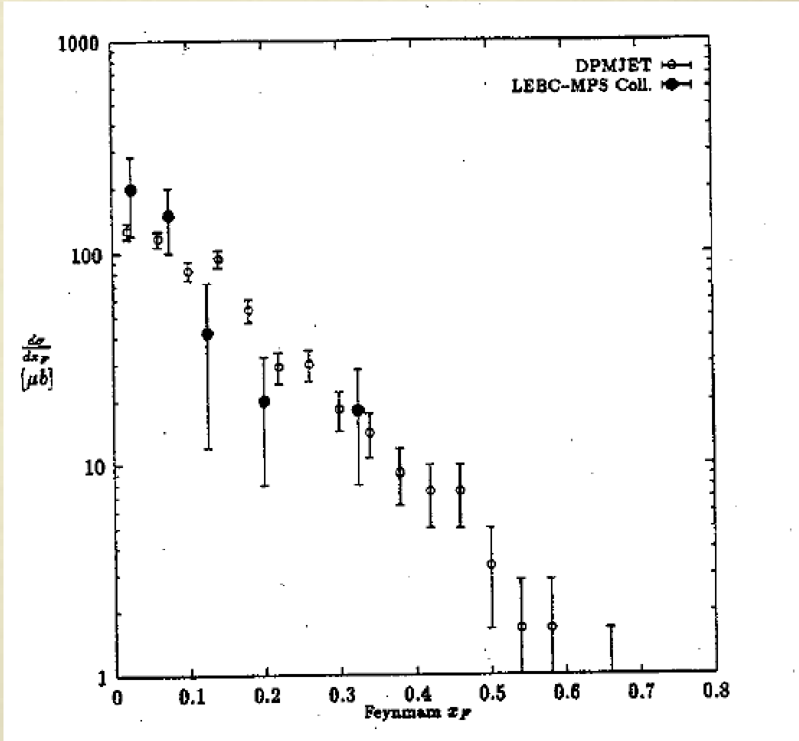

(harder, not seen in simulation)

At FERMILAB

- PRL (1988) p(800GeV/c)+p

$$a = 0.8 \pm 0.2\ (\text{GeV}/c)^{-2}.$$

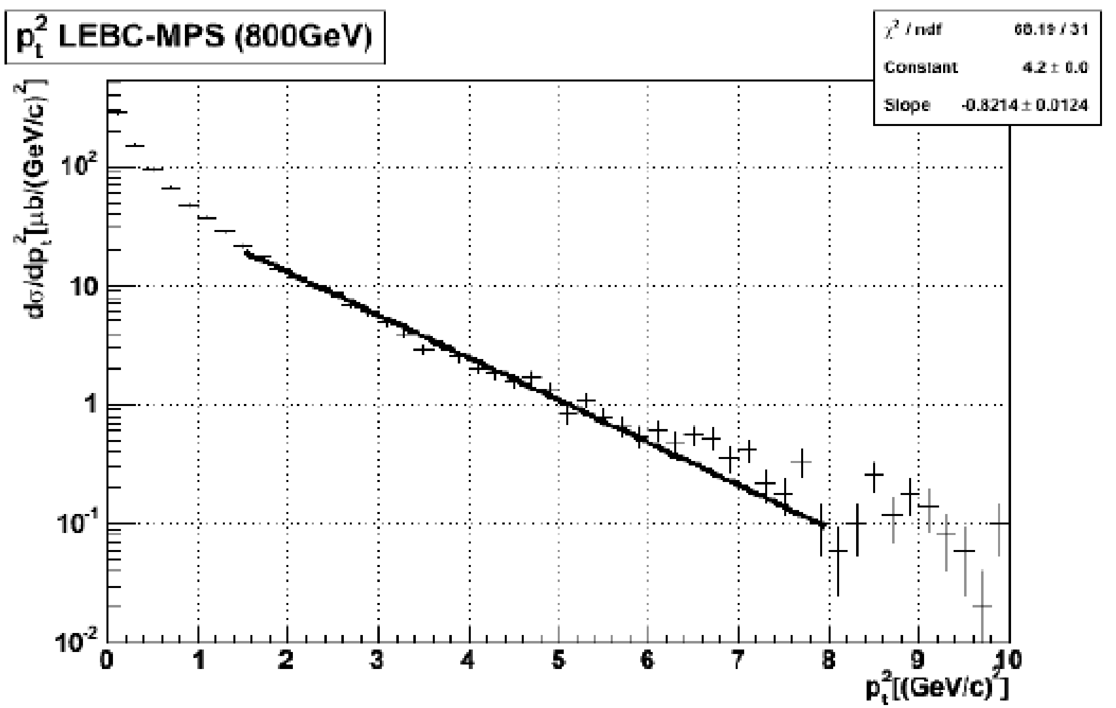

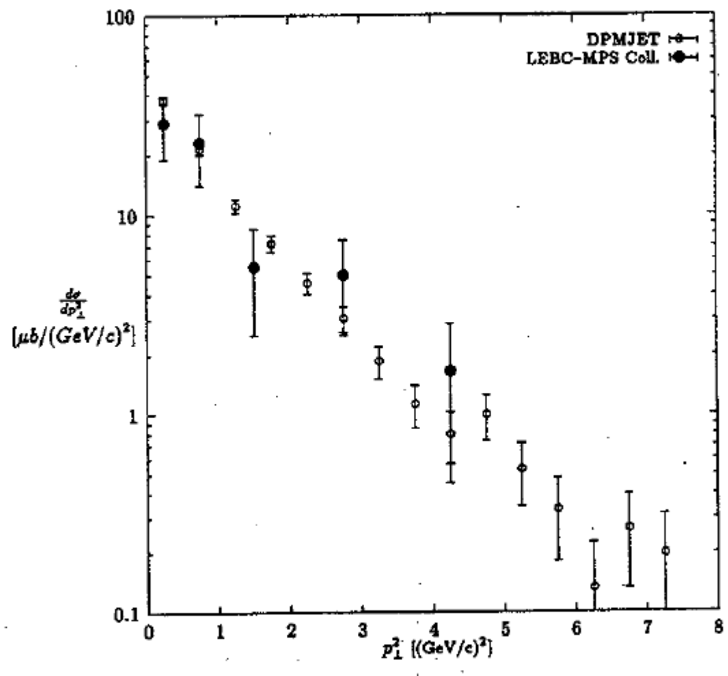

E791 (FNAL)

INVESTIGATE PROJECTILE FRAGMENTATION REGION

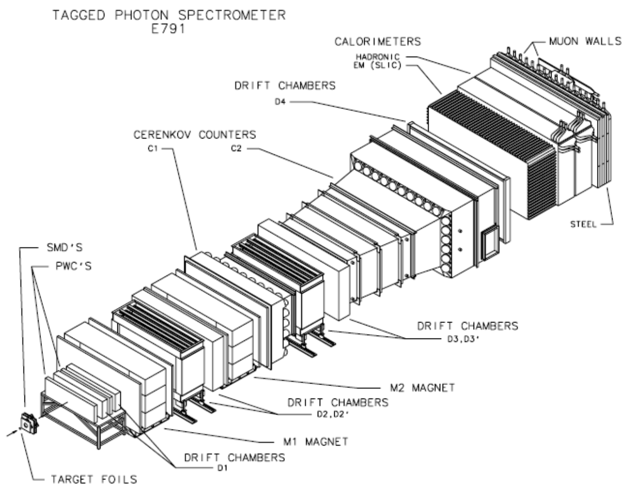

Fig. 2. The E791 spectrometer.

- 500GeV pi- on 4xCarbon + 1xPlatinum
- Total: 0.04% of pion interaction length
- Measured Lambda_{c} asymmetry, neutral D cross sections
- Target simulated as nitrogen due to CORSIKA constraints

http://ppd.fnal.gov/experiments/e791/docs/pubdocs/offline_doc_290.ps

http://ppd.fnal.gov/experiments/e791/docs/pubdocs/offline_doc_415.ps

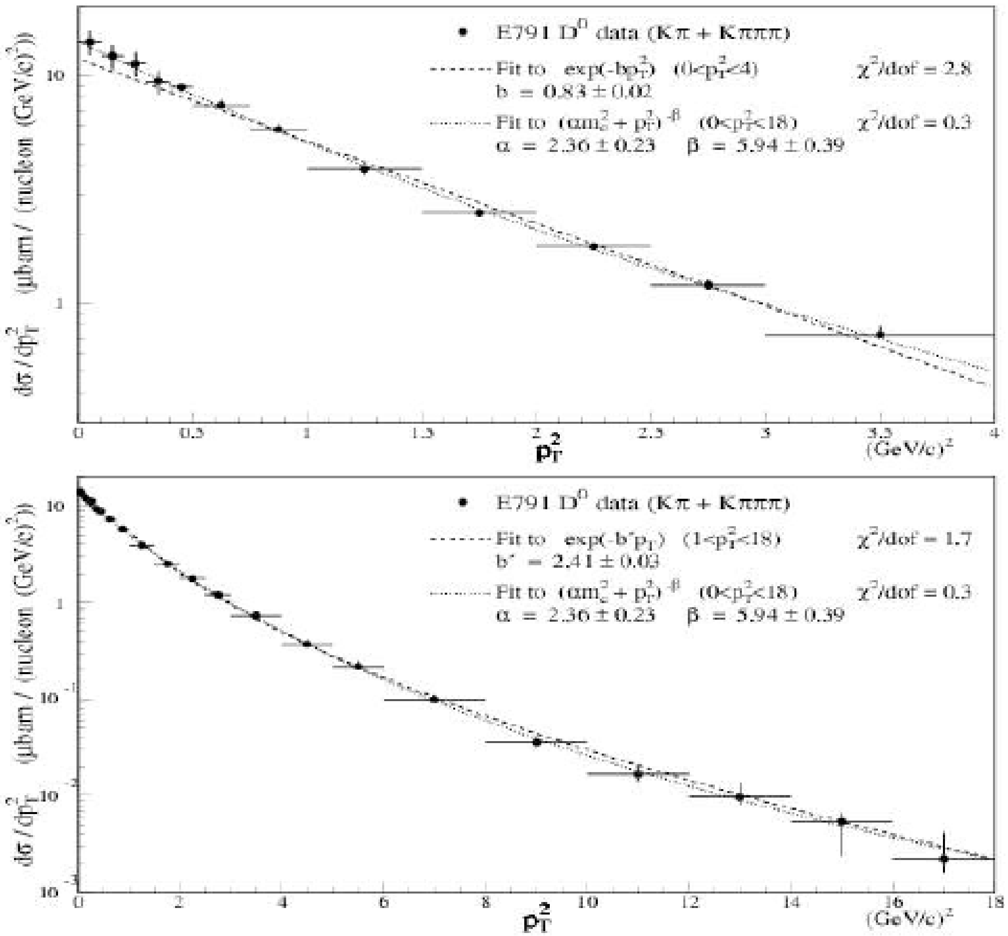

Fig. 4. Fits to the D^0+$\overline{D}^0$ p_T^2 differential cross section with the functions given in Eqs. 4 (dashed, top), 5 (dashed, bottom), and 6 (dotted, top and bottom). The top plot shows the range $0<p_T^2<4$ (GeV/c)^2 while the bottom plot shows the full range, $0<p_T^2<18$ (GeV/c)^2. Error bars do not include a $^{+11}_{-15}$% normalization uncertainty.

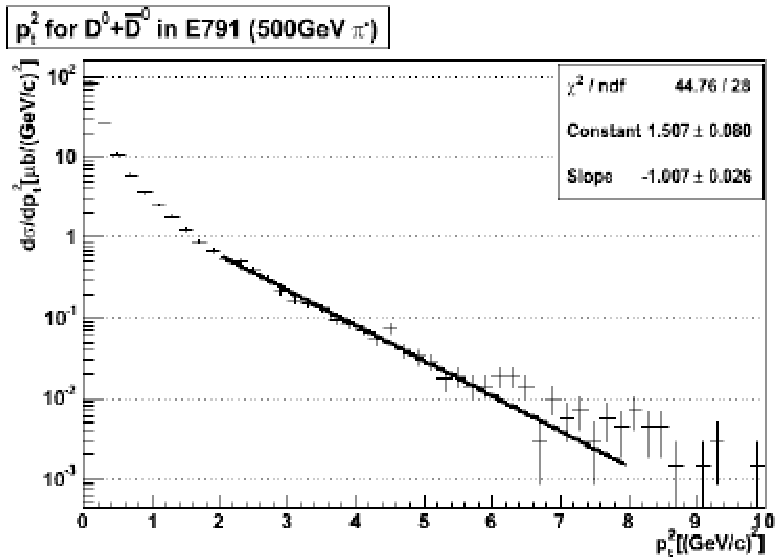

slope(exp): .83 +/- .002

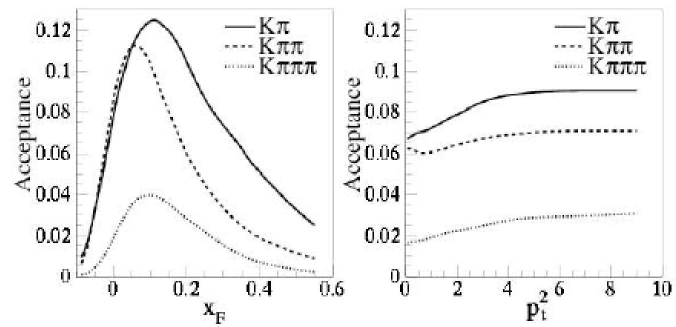

Fig. 3. E791 acceptance functions vs. x_F and p_t^2 for $K\pi$, $K\pi\pi$ and $K\pi\pi\pi$ candidates. The acceptance shown here is for a loose set of single-charm selection criteria. The p_t^2 acceptance is obtained for charm mesons with $-0.1 < x_F < 0.6$.

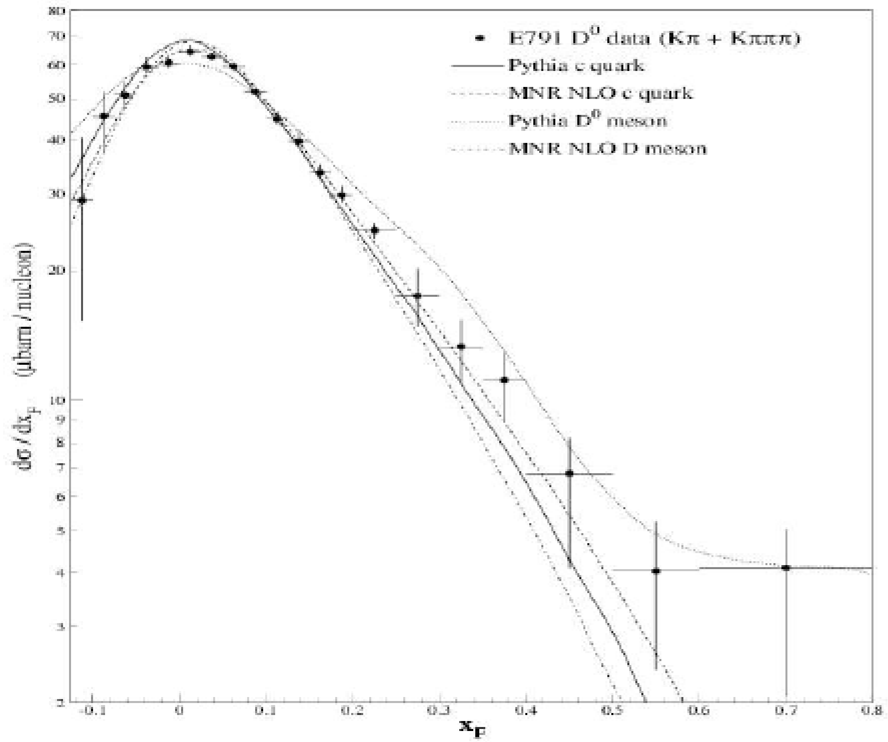

Fig. 5. The D^0+$\overline{D}^0$ x_F differential cross section compared to various theoretical predictions described in the text. The curves are normalized to obtain the best fit to the data in each case. Error bars do not include a $^{+10}_{-11}$% normalization uncertainty.

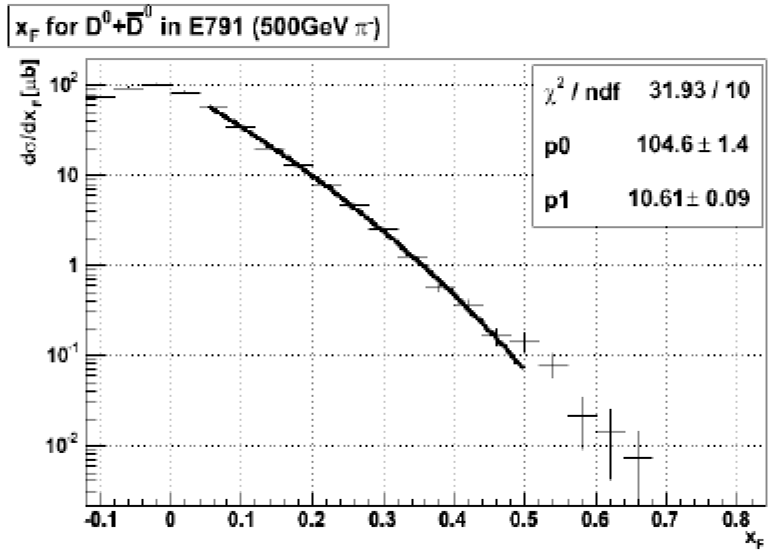

n = 4.61 +/- 0.19

much smaller!!!

Asymmetry

- Experimental measurements of single-inclusive x_F distributions for charmed hadrons find a behaviour that is harder than the perturbative QCD would predict

- Almost all experiments have observed the leading particle effect (production of fast particles which share a quark (or antiquark) with the beam)

D^0 Asymmetry

- Asymmetry in the target fragmentation region is smaller for proton target

Leading quark effect should favor D0
(ubar-d + uud) -> c-ubar
pi- + p -> D0

Selex

pi- 600 GeV

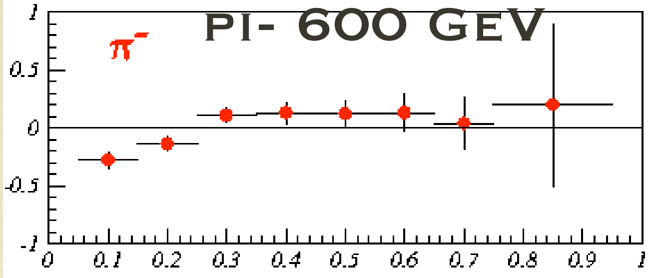

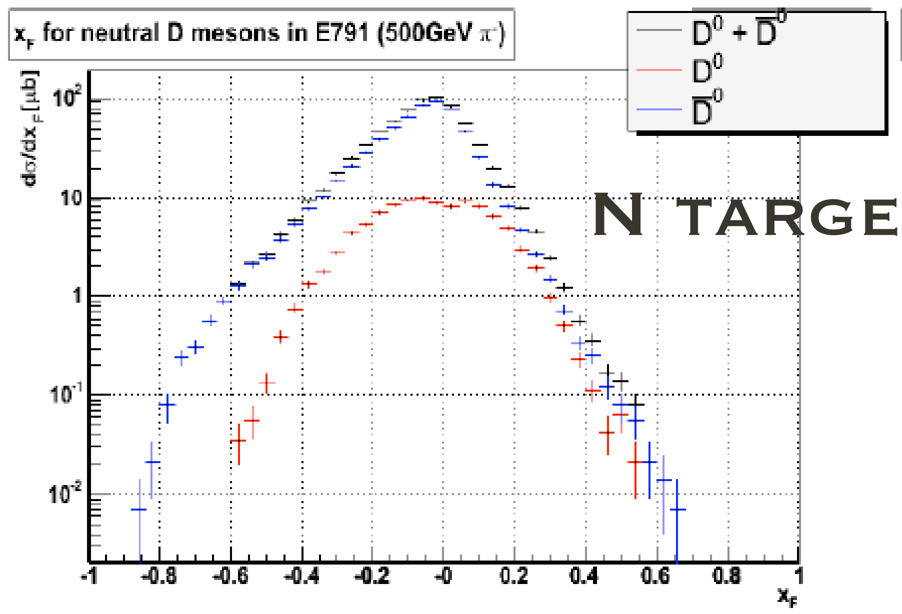

N target

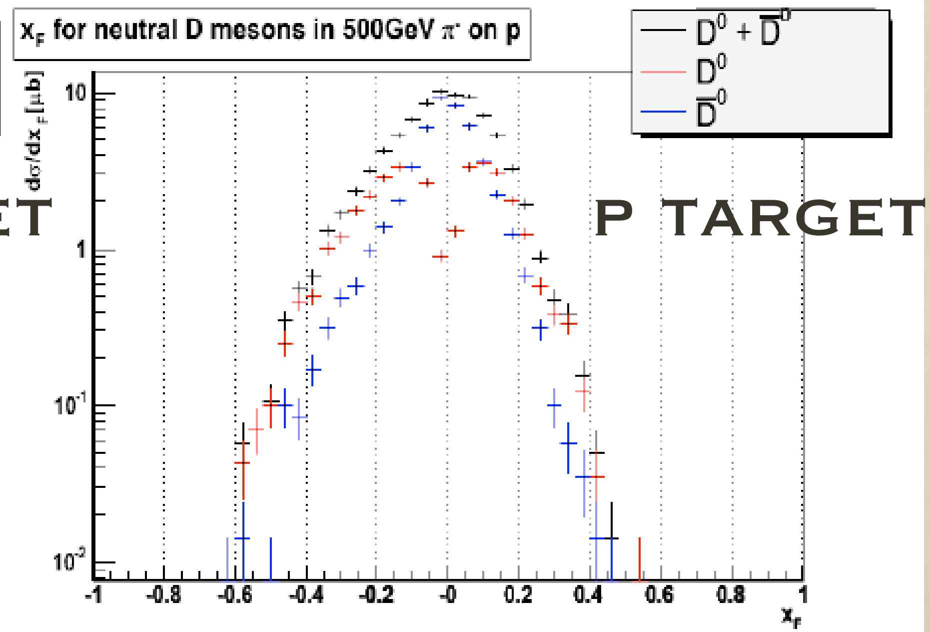

P target

$\overline{D}^0$ production from p beam shows no leading effect

SELEX (E781, FNAL)

- Fragmentation region: p, pi-, sigma beams (540-600 GeV)

- 540 GeV p- 5 target foils (3Cu+2C, 5% of proton interaction length): hadronic asymmetry of anti-lambda_c compared to lambda_c+ (hep-ex/0109017)

- CORSIKA 6.6 (1st interaction and resonances decay)

In corsika target is Nitrogen

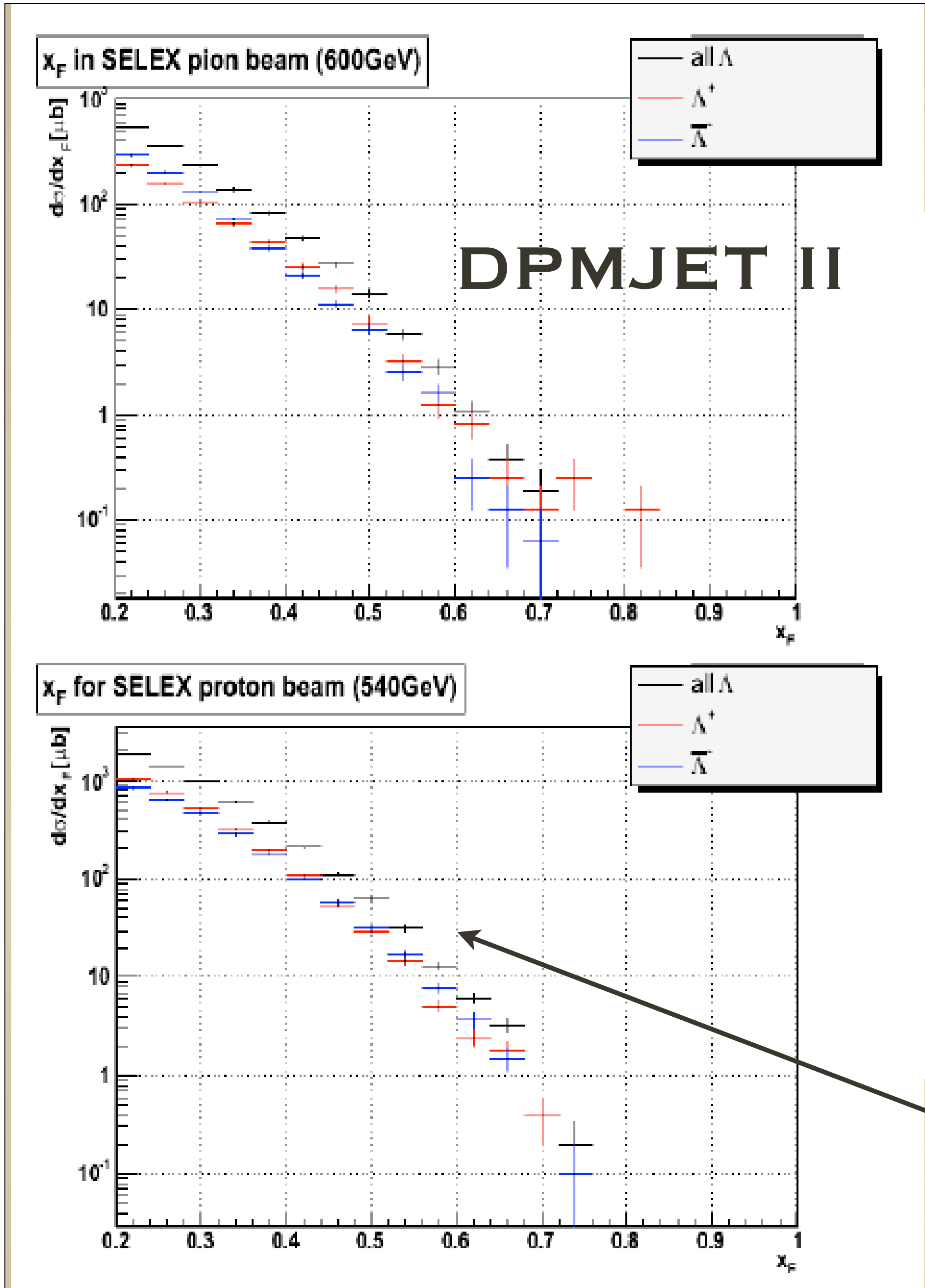

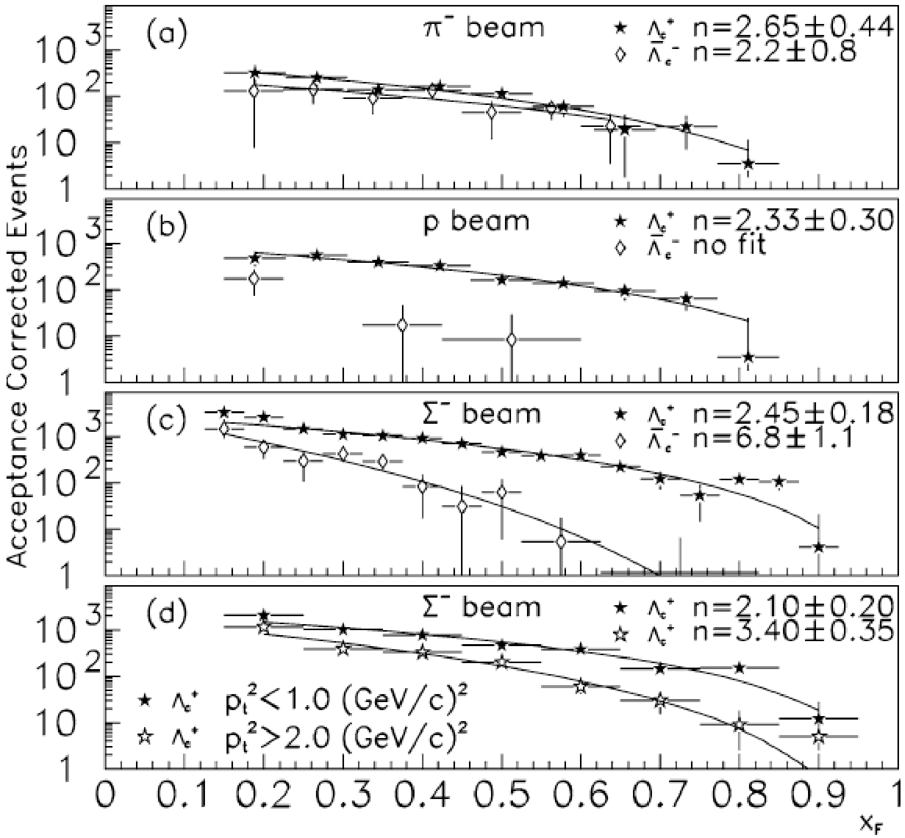

Distributions are harder for data and asymmetry is larger than in DPMJET

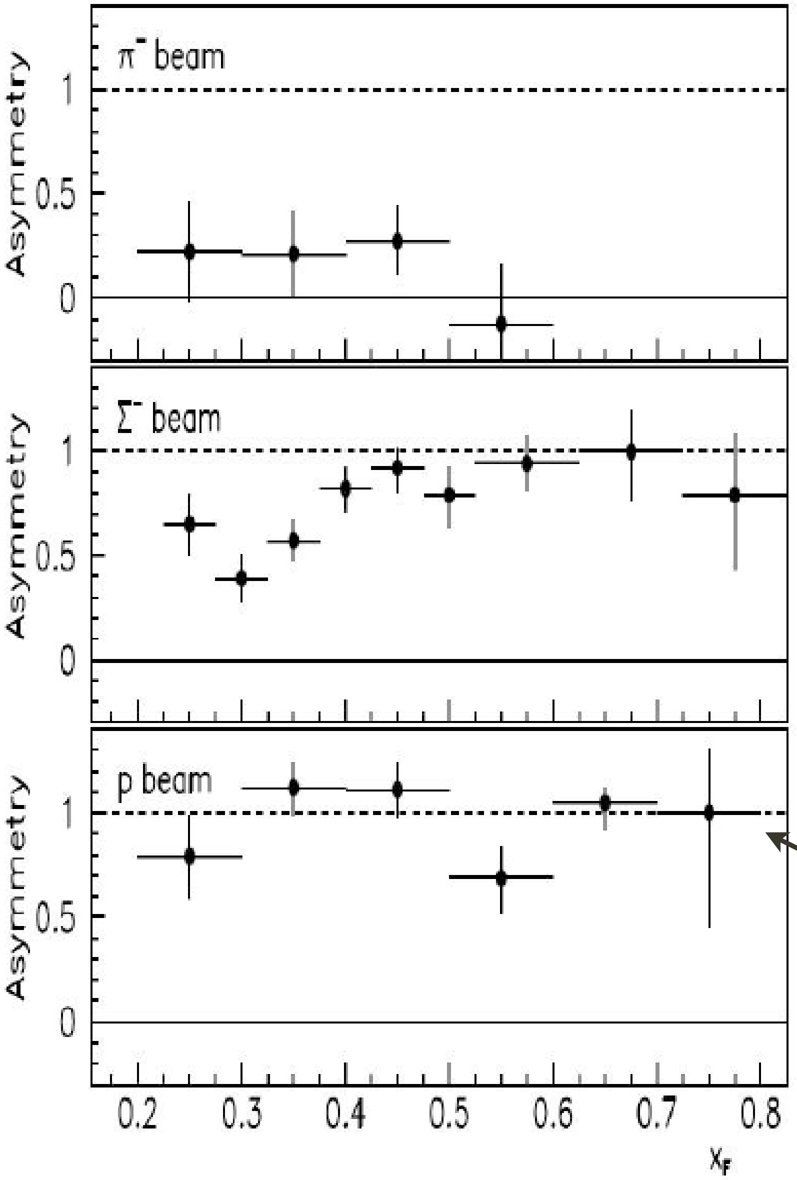

FIG. 5. Asymmetry for Λ_c production by π^- (top), Σ^- (center) and proton (bottom) beam.

$$A \equiv \frac{N - \overline{N}/r}{N + \overline{N}/r} \; ; \quad r = \frac{\bar{\epsilon}}{\epsilon}$$

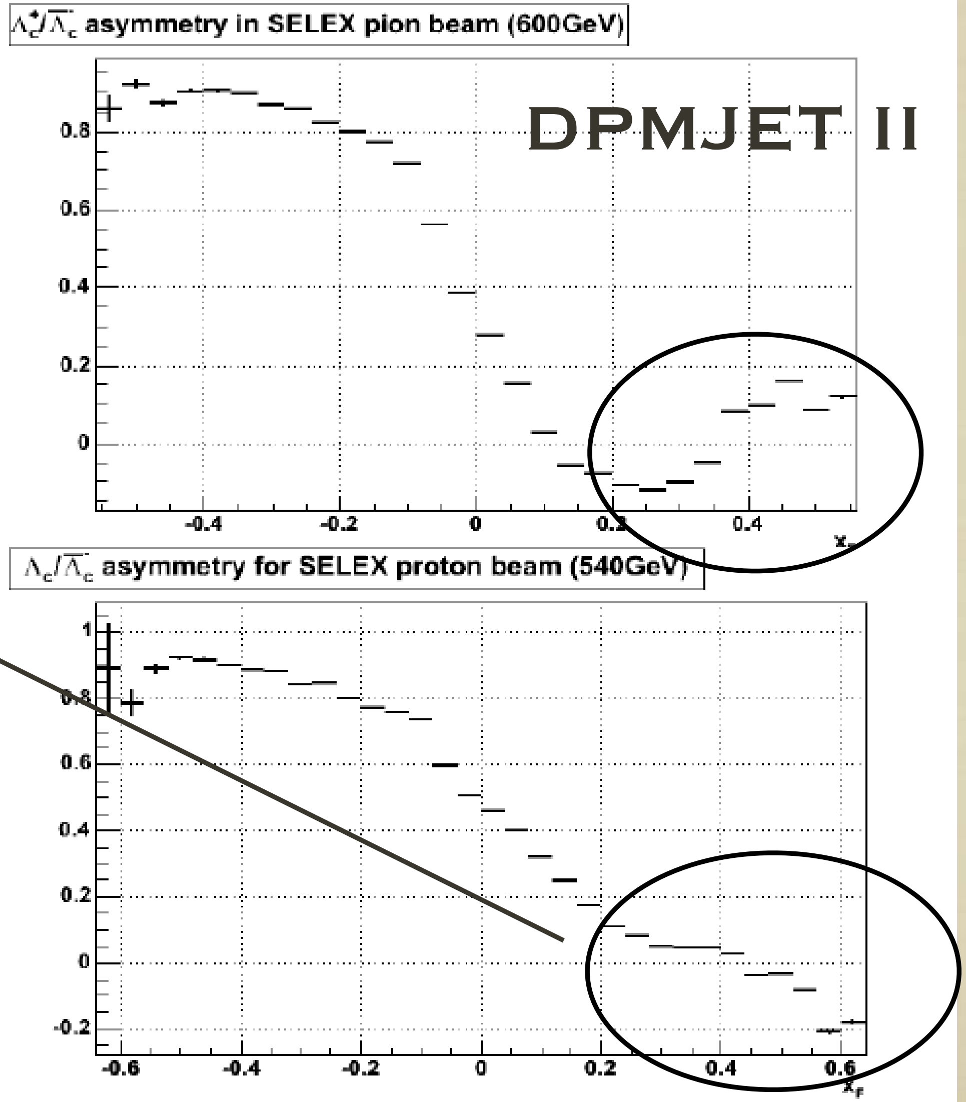

ASYMMETRY ON P TARGET

Same for proton target instead of nitrogen

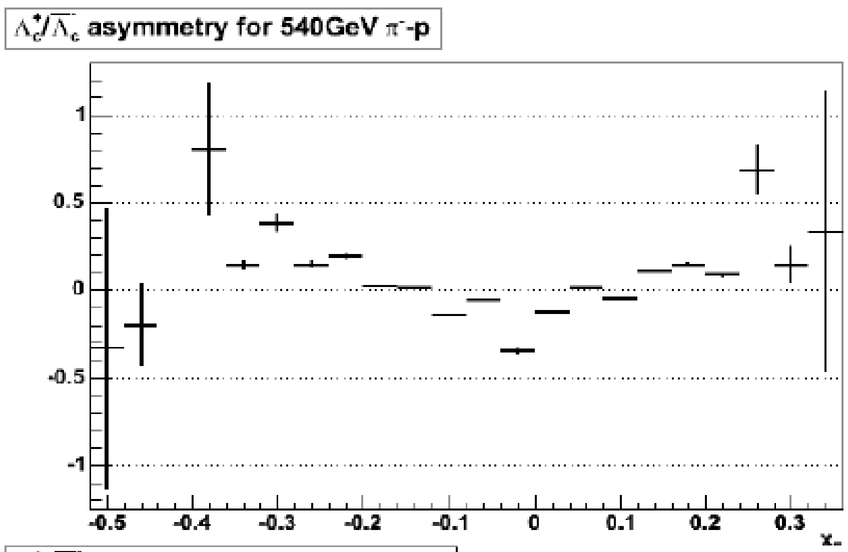

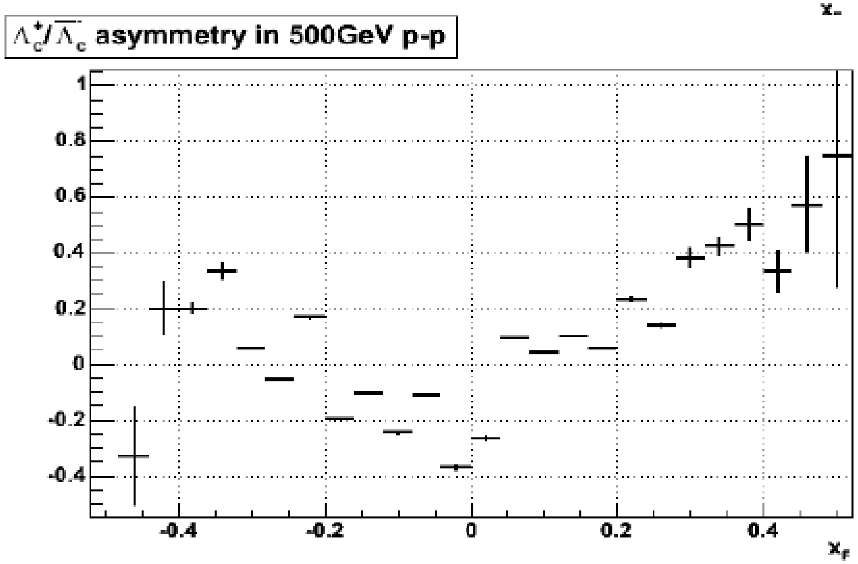

p-p and p-N differ: in p-N the charmed baryons and antibaryons are more similar to each other.
Asymmetries for baryons disagree with data because DPMJET needs same diquark fragmentation modifications for strange baryons and antibaryons.

FROM RANFT (STANDALONE DPMJET CONSISTENT)

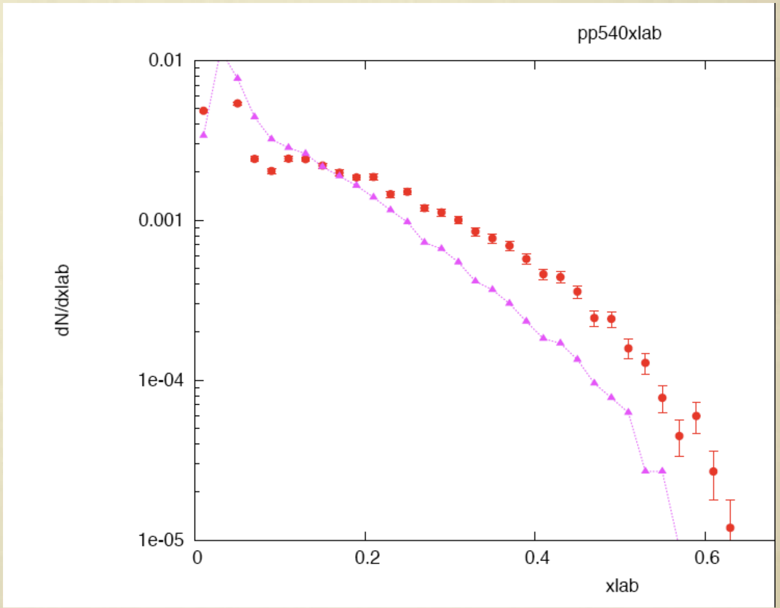

Conclusions

- IceCube and ANTARES will measure unprecedented statistics of atmospheric events
- the measurement of charm is challenging so signatures need to be investigated using full simulations
- DPMJET-II in CORSIKA, in FLUKA and standalone differ in a way which is not completely understood for p(1000TeV)+N
- charm data show harder x_F distributions than DPMJET-II
- Baryon asymmetries need some improvement in dpmjet-II